2017

The evolution of hardness and tribofilm growth during running-in of case carburized steel under boundary lubrication

Alexander David-Arthur Jenson
Iowa State University

The evolution of hardness and tribofilm growth during running-in of case carburized steel under boundary lubrication

by

Alexander D. Jenson

A thesis submitted to the graduate faculty

in partial fulfillment of the requirements for the degree of

MASTER OF SCIENCE

Major: Mechanical Engineering

Program of Study Committee:
Sriram Sundararajan, Major Professor
Scott Chumbley
Gap-Yong Kim

Iowa State University

Ames, Iowa

2017

TABLE OF CONTENTS

ACKNOWLEDGMENTS

I would like to thank my committee chair, Dr. Sriram Sundararajan, for committing his time and expertise throughout my graduate school experience. I would also want to thank my committee members, Dr. Scott Chumbley and Dr. Gap-Yong Kim for their guidance and support.

In addition, I would also like to thank my friends, colleagues, the department faculty and staff for making my time at Iowa State University a wonderful experience.

Finally, I must express my gratitude to my parents and to my fiancé for providing me with the encouragement and support I needed throughout my whole academic career. This accomplishment would not have been possible without them. Thank you.

CHAPTER 1. INTRODUCTION

Background and Motivation

Increasing efficiency and durability of gear and bearing systems has become an important goal as fuel efficiency for passenger and commercial vehicles has become more stringent because of economic and environmental concerns. Improvements in the efficiency between gear contacts lead to a decrease in frictional forces and failure modes, impacting multiple industries. To meet sustainable farming practices for a rapidly growing population, agricultural equipment powertrains need to reduce frictional losses, which are estimated to be about 10% of the total energy output, without compromising performance [1]. Efficiency concerns not only affect the passenger and commercial vehicle industry but renewable energy industries as well. For example, frictional forces within wind turbine gearboxes result in reduced electrical production, so increasing the efficiency and durability can make wind power more competitive. Mitigating frictional forces can reduce destructive failure modes like *pitting* and the considerable costs associated with early part replacement and unplanned shutdowns. This is especially important as new wind energy infrastructure growth is expected to grow at an increased pace [2]. Whether it is feeding the global population or moving toward a more sustainable energy future, improving gear and bearing efficiency and durability will have a significant impact on our society.

The branch of engineering which studies the friction, wear, and lubrication of interacting surfaces in relative motion is called tribology. Despite being officially defined in 1967, tribology has been in practice since the beginning of recorded history with records of early civilizations utilizing bearings and low friction of surfaces [3]. A notable contributor to the field was Leonardo da Vinci, who developed the basic laws of friction. Progress within tribology was slow, interrupted by the significant contributions by Osborne Reynolds in the late 18th century on hydrodynamic lubrication. Much of the knowledge gained within the field took place after World War II and when advanced measurement techniques allowed tribologists to better understand the interactions

occurring at the micro- and nano-scale levels. Understanding the mechanisms which lead to undesired wear and friction have vast economic saving potentials. An analysis of worm gear drives in the United States found switching the all to a lubricant which raised the mechanical efficiency by 5% had the potential to save about $0.6 billion (1987) per year [4]. The impact of this incremental improvement is attributed to the sheer volume of tribological systems used throughout the U.S. and other countries, and dictate the necessity for many engineers, not just tribologists, to have some knowledge of tribology.

Due to a combination of rolling and sliding, contacting surfaces undergo wear which leads to stress-related failure modes like fatigue wear. For example, repetitive contact between gear teeth surfaces causes collisions between asperities, the peaks in surface roughness, on adjacent surfaces, even under lubricated conditions. The repeated contact fatigue introduces cracks because of the stresses generated between two elastic bodies pressed together. Cracks can originate at the surface and subsurface depending on the rolling and sliding conditions and form pits on the surface. This pitting is attributed to various failure mechanisms discussed in Chapter 2. In addition to failure, asperity contact contributes to loss of efficiency. Many techniques are utilized to decrease surface roughness and asperity contact, and thus, increase efficiency. Xiao et al and Petry-Johnson et al. showed a reduction in gear tooth surface roughness was significant in reducing the mechanical losses for high speed and torque conditions [5,6]. Many other studies are dedicated to characterizing and increasing the mechanical efficiency between contacting surfaces by improving lubricants and decreasing surface roughness [7–11].

Modern machines utilize components which have superior surface finishes and clean lubricants which prevent the origination of surface cracks, but subsurface cracks dominate rolling contact fatigue failures. Manufacturers main defense against crack growth in contact fatigue is via the case- and through- hardening. Through-hardening is used on medium carbon (0.25% - 0.5%) and high carbon (0.5% - 1.0%) steels and case hardening is used on mild carbon (less than 0.25%) steels. Hardening occurs during heat treating when the steel is cooled rapidly or quenched which leaves behind residual

stresses. Residual stresses greatly inhibit the propagation of microcracks through the treated surface [12] and fatigue lives of components can be extended when compressive residual stresses are present [13,14]. However, these treatments are cost and energy intensive and these stresses can be affected by the plastic deformation which takes place during contact fatigue. Plastic deformation can generate positive effects during contact fatigue through work hardening. Working hardening can occur naturally during the regular operation of components, albeit uncontrolled. However, if work hardening could be utilized before the normal operation of bearing and other rolling/sliding components, it could produce more predictable material performance.

To promote the optimal contact between the virgin surfaces components, manufacturers and engineers utilize the process of running-in. This initial wear and plastic deformation of the surfaces only lasts for a short period and concludes when a mild wear or frictional steady-state is reached. No preferred running-in strategy has been agreed upon because many approaches are found among researchers and manufacturers. It is common to that run-in takes place at some fraction of the target load (20% to 80%) and time (75,000 to 600,000 cycles). Much of the gear efficiency research performed still has not fully characterized the details of run-in and only utilize it as a starting procedure for tribotests [6,8,9]. Additionally, there is a gap in understanding all of the changes which occur during the initial phases of run-in which was identified by Blau [15]. Research has shown how the surface geometry evolves under some conditions, but few studies focus on subsurface microstructure changes. Berthe et al. observed after ten cycles of run-in, the roughness topography showed little change but local plastic deformation of the asperities stopped [16]. It is not clear whether this plastic deformation is causing significant work hardening during this short period of time, but it has been shown at higher cycles [17].

Manufacturers of gears, bearings, and other tribological components are tasked with making products which are more efficient and durable so they can meet higher operational and environmental demands. Power and efficiency losses make machines less competitive and destructive failures can set back entire operations. Running-in of

gears and other rolling elements promotes smooth contact surfaces and minimizes the initiation of surface cracks, however, subsurface cracks still prorogate from contact fatigue. Heat treatments can help strengthen the materials, but are expensive, and even when they are used, pitting still occurs. Work hardening occurs naturally during run-in and the normal operation of components, so if run-in procedures could be designed to control the hardness gains during the process, it would help make components more resistant to pitting. Much still needs to be explored during the initial phases of running-in, especially how the hardness of materials changes because of their operational conditions. Crack initiation during contact fatigue may not be completely avoidable, but understanding the transformations which occur will help design more efficient and durable components.

Research Objectives

The first objective was to conduct a literature review to develop a strong scientific understanding of the mechanisms and characterizations of running-in as it is understood process today. The review allowed for the documentation of materials, methods, and procedures for conducting controlled running-in tests. Materials and methodology were chosen based on components utilized throughout industry and previous research, so comparisons could be made between experimental observations and those seen throughout the body of research. The next objective was to observe the evolution of hardness during running-in and how the property varied under different load and roughness conditions. The final objective was to evaluate the experimental data and provide scientific reasoning for any observed trends among the different conditions. The findings of this study can be used in conjunction with existing data in this field to help guide future work and assist in characterizing the initial stages of running-in for industrial and experimental applications.

Research Approach Summary

The databases *Web of Science* and *ScienceDirect* were used for accessing and compiling most of the literature used to compose a literature review. As will be shown in the upcoming section, there are several methodologies for conducting run-in. Therefore, materials, operating conditions, and measurement techniques were chosen with respect to their viability and real-world applications since the motivation behind this research is improving tribological components present in numerous industries.

The piece of equipment used for this study was a Micro Pitting Rig (MPR) designed by PCS Instruments. The MPR is a computer controlled three-contact disc instrument where three, 'counter face' rings are evenly spaced around a central, smaller diameter 'roller' as seen in *Figure 1*. This arrangement allows the roller to undergo numerous contact cycles in a relatively short amount of time. The onboard processor for the MPR allows for the automatic control of speed, slide-roll ratio, and temperature. Two servo-control motors allow for various combinations of slide-roll ratio and entrainment speed. The conditions held constant for each test are shown in *Table 1*.

Figure 1. Micro Pitting Rig (MPR) test chamber with three 'rings' and one central 'roller' (PCS Instruments) [18].

Table 1. Conditions used for every test. Parameters resulted in boundary lubrication for all conditions.

Parameter	Value
Time	150 minutes
Contact Cycles	109,669 cycles
SRR (Eq. 1)	20%
Entraining Velocity	0.17 m/s
Spin-off Temperature[a]	80 °C

[a] Spin-off Temperature was measured by temperature probe inserted into the test chamber with the tip of the probe placed close to the contact region

$$SRR\ (\%) = \frac{U_1 - U_2}{{}^1\!/_2 (U_1 + U_2)} \quad (1)$$

Preliminary hardness testing was performed on the 'roller' which was put under a run-in procedure typical for low-speed, high-torque applications. This testing indicated hardness increased after the running-in procedure, but the extent of the hardness increase was different for the varying load and roughness conditions. The selected material for the MPR 'rings' and 'roller' was AISI 16MnCr5 (SAE 5115) steel that was case-carburized and a finish ground with a circumferential surface texture lay direction. 16MnCr5 was chosen because of its wide use as a material for high-performance ball and rolling element bearings. Carburization of steel produces a material with varying microstructure as a function of depth [19]. The surface region will contain a higher distribution of carbides within the steel matrix and this distribution will decrease with depth. The carbides are harder than the rest of the steel matrix, and therefore, the surface will typically be harder at the surface and decrease in hardness with depth [20]. Information on 16MnCr5 steel's microstructure is limited, but reports indicate 20 vol% of retained austenite is present in similar 5120 steel with no residual carbides [21]. However, in another study, retained austenite and residual carbides were present in 4118 steel, but the extent of which, was not reported [22]. The initial roughness and case depth of the rollers and rings can be seen in *Table 2*.

Table 2. Roller and ring surface roughness and hardness specifications (per manufacturer).

Part	Roughness, Ra (μm)	Case Depth (mm)
Roller (specimen)	0.15 ± 0.05	0.9 min
Ring (smooth)	0.125 ± 0.025	0.9 min
Ring (rough)	0.45 ± 0.05	0.75 - 1

The oil used in this study was an API Group II base oil with ZDDP anti-wear and other additives. One of the additional additives was a viscosity index (VI) improver, so the oil was sheared prior to testing by running it through a piston pump for 48 hours. Shearing the oil prior to testing lowers the viscosity of the oil, so it does not do so through the course of testing. Group I base oils have traditionally dominated the market in terms of their use, but Group II and Group III oils are becoming more popular because of their superior properties. Group II base oils have greater resistance to oxidation than Group I oils because of their high content of saturated hydrocarbons [23]. This helps the oil maintain stability at high operating temperatures like those found in engines [1]. The MPR utilizes a dip lubrication system where the two lower rings are partially submerged in the oil. The oil is heated via an electric cartridge and a temperature probe is inserted into the test chamber and positioned near the contact region (*Figure 2*).

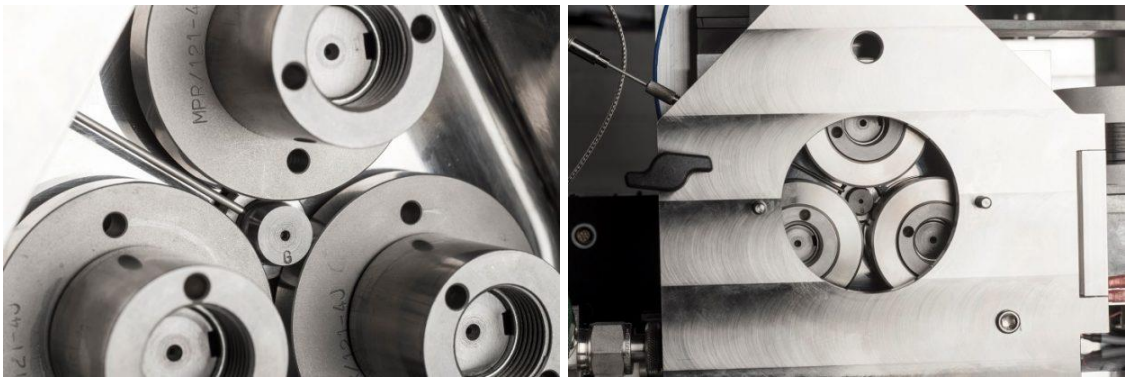

Figure 2. (Left) Positioning of the temperature probe within the MPR (PCS Instruments) test chamber. (Right) Test chamber with the door closed [18].

The test chamber is arranged so that the test can be stopped (unloaded and rotation stopped) so the central roller can be removed and inspected without having to remove the rings or draining the lubricant (*Figure 2*). This feature was utilized to observe the evolution of the roughness and hardness of the roller at various intervals. After a test interval, rollers were removed and cleaned with 70% isopropyl alcohol to remove any residual lubricant and then an optical profilometer was used to measure the roughness of the wear track and view the topographical structure. The hardness profile was measured using a Vickers microhardness indenter. For tribofilm analysis, energy dispersive spectroscopy (EDS) was used to analyze the chemical composition of the case of the roller after undergoing wear.

The tools and experimental instruments used for performing tests and analysis of the roughness and hardness evolution were chosen based on their proven success in current literature relevant to this field of study and their availability at Iowa State University. Any instruments or materials deemed necessary for this study, that were not already available at Iowa State University, were purchased.

Thesis Organization

The thesis is organized into five chapters. Chapter 1 has introduced the research problem. Chapter 2 consists of a literature review which provides definitions, measurement techniques, and classification systems for running-in, surface roughness, contact mechanics, work hardening, and lubrication. The methods for conducting running-in will also be reported in Chapter 2.

Chapter 3 consists of the manuscript accepted to the journal *Wear,* The *effect of contact pressure and surface texture on running-in behavior of case carburized steel under boundary lubrication*. The experimental work and writing of this paper was performed by Wagner with Jenson contributing hardness analysis and writing.

Chapter 4 consists of the manuscript to be submitted to the journal *Wear* titled: *The evolution of hardness and tribofilm growth during running-in of case carburized*

steel under boundary lubrication. The experimental work and writing of this paper was performed by Jenson with Sougata Roy contributing tribofilm analysis and writing.

The thesis will be concluded with Chapter 5 in which conclusions from these studies will be reported and recommendations for further research.

CHAPTER 2. LITERATURE REVIEW

Running-in

Running-in is the initial wear and plastic deformation of the surface, starting with the conditions after manufacturing. It is understood that run-in is achieved when a steady-state phase of friction or mild wear is reached, but the smoothening of the surface does not necessarily occur simultaneously with the steady-state coefficient of friction [24]. The transformation of wear and friction are characterized by changes in the thin surface layer's conformity, oxide film formation, material transfer, lubricant reaction product, martensitic phase transformation, and subsurface microstructure reorientation [25]. These numerous changes in the surface affect the frictional running-in behavioral curves, eight of which were identified by Blau when analyzing data from previous research done in the field [15]. Since the surface topography, load, speed, and environment have such a significant effect on the run-in process, parameters must be carefully designed to produce controlled running-in of surfaces.

Running-in was initially addressed by Abbot and Firestone whose influential study in 1933 outlined the idea of bearing area curve and led to an understanding of the changes in surface topography during contact [26]. They described as two new surfaces initially come into contact, they touch at the highest peaks of the surface or asperities. When these surfaces undergo running-in, the peaks are gradually worn down and the surfaces become smoother. Initially, the contact area between surfaces is small, but as they undergo running-in, the load is distributed over a wider area and the rate of wear decreases [26]. Running-in promotes the suitable fitting of new parts, like those found in transmission, engines, and gearboxes. Contact loads, temperatures, and wear can be increased inadvertently if the optimal alignment is not achieved during running-in, so it is important to consider the how surfaces develop at the micro and even nanoscale levels.

Running-in Methodologies

Running-in is utilized as a starting procedure to condition parts in situ. In the past, consumers needed to follow strict running-in procedures themselves, but advancements manufacturing and lubrication have lessened the burden. However, certain systems still very much rely on running-in to increase the life of components. In the case of piston rings in high-pressure hydrogen compressors, controlled run-in can increase the life from 24 hours to two years [27]. This shows minute changes in micro-geometry can influence the service life, so careful attention must be given to the initial wear, plastic deformation, and stress states in the design of running-in procedures [28].

Research, like that done by Roy Chowdhury et al. observed how varying load and speed conditions of running-in affected the wear and plastic deformation of surfaces. They observed higher loads had a greater impact on the surface smoothening more so than increased speeds and determined smoothening was most likely caused by a combination of abrasion and plastic flattening [29]. From this work, it is clear surface asperities decrease, but the extent to which is due to plastic deformation in not quantified. According to Jacobson, surfaces in contact experience new running-in conditions as soon as conditions change [30], so careful consideration must be made when designing controlled running-in for a variety of loads, speeds, and environmental conditions.

No preferred running-in strategy has been agreed upon because many different approaches are found among researchers and manufacturers, but in general, vary load, speed, and duration. Kahraman et al. set their run-in for 60% of the maximum gear load for 360,000 cycles using ground and super-finished gears [6]. Andersson used 300,000 cycles to run-in hobbed and green-shaved gears [31]. Yoshizaki et al. utilized step-wise loading to bring the load from 9% to 100% of the maximum load [9]. Akbarzadeh and Khonsari developed a running-in model which showed varying speed, load and surface lay affected both steady state running-in and friction response [32] These and other research performed does not fully characterize the details of run-in and only utilize it as a starting procedure for tribotests [8]. Blau argued not enough attention was given to

the initial phases of running-in and a lack of detailed studies existed to fully interpret the mechanisms occurring during this transition [15].

Surface Topography

One aspect of running-in which is thoroughly observed is the change in surface topography, the study of the geometric shape of a surface. When Earth is seen from space, it appears as a smooth sphere, but observing it from the surface reveals peaks and valleys. The same can be about ball bearings, albeit at different scales. When viewed at the micro and nanoscale levels, waviness and roughness are revealed in the surface. Waviness is the deviation from the form, or basic shape, intended in the manufacturing of the surface (i.e. a spherical ball bearing or cylindrical involute gear tooth) resulting from the dynamic instability of the machine or tool being used. Surface roughness is the shorter deviations from the perfectly smooth surface created by the chip generation process in machining components. Waviness is measured via Gear Measurement Instruments and surface roughness can be measured using a variety of equipment via contact (diamond stylus) or optical methods (white light interferometer). Since it is difficult to differentiate between the cut-off between waviness and surface roughness Whitehouse recommended basing measurements off the magnitudes of specific parameters rather than the manufacturing features and machine processes [33].

Surface roughness parameters are classified as spatial, amplitude (averaging or extreme), or hybrid. The typical industry parameters are the arithmetical mean deviation of the profile (Ra), the extreme value parameters of ten-point height (Rz), the maximum height of the profile (Rt), and maximum profile peak height (Rp). Some other parameters found in research studies are: root mean square roughness (Rq) and the measures of the distribution density of profile deviations, such as skewness (Rsk) and kurtosis (Rku). Despite these roughness parameters frequent use in industry, they do not provide information on the shapes of the asperities which Whitehouse and Archard sought to quantify by their mean radius of curvature [34]. During the running-in process, the curvature of the asperities is flattened via a combination of wear and plastic

deformation shown by Berthe et al., Akbarzadeh and Khonsari, and Clarke et al. [16,35,36]. However, it is unclear how much the flattening is attributed to the wear and plastic deformation but agreed that during running-in, it is a rapid process.

Contact Mechanics

When two contacting surfaces are under load they will deform either plastically or elastically depending on the magnitude of the load and material properties of the surfaces. In tribological systems like gears, cams, seals, ball bearings, etc., the surfaces are non-conforming, resulting in small contact areas and high pressures between the surface asperities. It is crucial to know the stresses generated from these contacts so machines and their components can be designed and manufactured appropriately. The formulae used to calculate these stresses were developed by Hertz in 1881 and later published in his watershed paper *On the contact of elastic solids* [37].

Hertzian contact theory is by its assumptions, one being the contact between stationary bodies. A major consideration when running in surfaces is to analyze the solid-to-solid contact under sliding to help understand the wear and friction between surfaces. Work by Al-Tubi et al. discusses how sliding contact may magnify the development of micropitting due to the surface layer being pulled from the pitch line for contacting gears [38]. Another assumption made in the Hertzian contact model is the contact between two bodies is made from two perfectly smooth surfaces. The true contact area formed between two rough surfaces is actually a distribution of micro-contact area which increases with load, first described by Greenwood and Williamson [39].

For the present study, the contact made between the 'roller' and 'rings' form an elliptical contact area are calculated from Deeg [40]. *Equation 2* is used to approximate the elliptical contact radii, a and b, where p is the normal force, R is the effective radius, and k is the root of the transcendental equation. θ_1, θ_2, and Ω represent contact angle geometry. *Equation 3* is used to approximate Hertzian contact pressure, $(Z_z)_{max}$.

$$a = \left[\frac{3\,p}{4\,\pi}\frac{(\theta_1+\theta_2)}{R\,sin^2(\Omega/2)}\int_0^\infty \frac{dt}{\sqrt{(1+k^2\,t^2)^3\,(1+t^2)}}\right]^{1/3} \quad b = \left[\frac{3\,p}{4\,\pi}\frac{(\theta_1+\theta_2)}{R\,sin^2(\Omega/2)}\int_0^\infty \frac{dt}{\sqrt{(1+\,t^2/k^2)^3\,(1+t^2)}}\right]^{1/3} \tag{2}$$

$$(Z_z)_{max} = \frac{3\cdot p}{2\cdot\pi\cdot a\cdot b} \tag{3}$$

Work Hardening

During the running-in of surfaces, it is understood that some work hardening can occur as a result of the plastic deformation between the surfaces [15]. Generally, studies have not focused on how hardness changes within materials which undergo running-in but work like that done by Hirano et al. suggest controlling this effect can increase resistance to pitting [41]. Burbank and Woydt found the cold work hardening of high-performance steels helped increase the operational lifetimes of the materials [17]. Their results showed for 20MnCr5 steel, hardness was increased approximately 60 HV (using 200 gf indenter load) within the wear track by running samples at a maximum pressure of 3.8 GPa for 10,000 cycles. They also analyzed the residual stress profiles which indicated evidence of work hardening. Other work by Dommarco et al. looked specifically at levels of residual stresses and retained austenite following rolling contact fatigue and more resistance to fatigue from materials with higher volume fractions of retained austenite [42]. They observed the evolution of residual stresses increased with the number of cycles when running under a contact pressure of 3.6 GPa. A study by Kang et al. suggests the increase in hardness they observed in their experiments at happened earlier than 10^7 cycles with under operating conditions of 3.7 - 5.6 GPa [43]. This could indicate running-in experiments may develop an increase in hardness at the early stages.

Lubrication

When two surfaces move relative to one another with sufficient velocity and under lubricated conditions, a load carrying film can form [23]. This hydrodynamic film separates the adjacent surfaces and protects them from wear under conformal contact. Interestingly, in highly loaded non-conformal contact, where surface roughness is

similar in magnitude to that of film thickness (0.1 to 1 µm), wear is still mitigated. It was proposed by Ertel and Grubin that the mechanism which allowed this was attributed to the combination of hydrodynamics, elastic deformation and an increase oil viscosity due to the high pressures [44]. In systems under intense contact stresses, the hydrodynamic pressure elastically deforms the surface asperities, vastly reducing the wear and friction of the system. This model is referred to as elastohydrodynamic lubrication or EHL.

Evaluation of EHL film thickness assumes the surfaces in contact are flat, but in applications like running-in, the surfaces are covered in varying features that affect the generation of these films. Dowson showed their components operated without failure when the calculated minimum EHL film thickness (0.2 to 0.4 µm) is of the same magnitude as the surface roughness of the two surfaces [45]. The variation in film thickness as a function of surface roughness is an important parameter developed by Tallian and important in the design of running-in experiments [46]. This ratio of minimum film thickness to composite surface roughness is defined by *Equation 4* where h_0 is the minimum film thickness and σ_A and σ_B are the RMS surface roughness of bodies A and B.

$$\lambda = \frac{h_0}{\left(\sigma_A^2+\sigma_B^2\right)^{1/2}} \tag{4}$$

If λ is less than 1, it can result in surface smearing, deformation, and wear. For λ values between 1 and 1.5, extreme plastic deformation of the surface asperities or 'glazing' occurs. Between λ values 1.5 and 3, some nondetrimental glazing can occur, but it can eventually lead to pitting. Values above 3 and 4, result in minimal wear and full EHL film separation respectively. Most components operate sufficiently in low λ conditions (≈1), but even with EHL, contact between the asperities can still occur because of ununiform roughness. In scenarios like running-in, the load is shared intermittently by the lubricant and asperities referred to as 'mixed' or 'partial lubrication'. This partial EHL was developed by Johnson, Greenwood, and Poon [47].

Tribofilms

Lubricants commonly feature friction modifiers and anti-wear additives to help extend the life of components in tribosystems like engines and transmission. One of the most common and effective anti-wear additives is dialkyl dithiophosphate (ZDDP) because of its superior anti-wear, extreme pressure, and antioxidant properties. During tribochemical tests, ZDDP is shown to form tribofilms on the surfaces of the materials it lubricates [48–52]. Of the research performed, most acknowledge a similar pattern in chemical behavior but attribute slightly different mechanisms for the formation of films. Since the formation of these tribofilms initiates in rolling-sliding contact applications, some researchers believed it was caused by increased surface roughness [53,54]. Other work suggested the growth of the films can be additionally attributed to the high, localized contact pressures caused by the asperity contact between surfaces [55,56]. However, it is generally understood ZDDP undergoes a decomposition reaction which increases with temperatures above 150 °C.

Researchers can determine the composition of the tribofilms deposited using a variety of techniques. In the 1970's, the vacuum-based, surface analysis techniques like XPS (ESCA), Auger, SIMS and EDAX were used to study the chemical composition of ZDDP anti-wear films and revealed they formed a patchy structure on steels [57,58]. Based on these techniques, the films were estimated to be 50 – 100 nm thick [59]. Depending on conditions like load, rubbing time, and ZDDP concentration, the thickness of the films were shown to reach around 140 nm [60,61]. Work by Parsaeian et al. showed tribofilm thickness was inversely affected by relative humidity by varying humidity levels during rubbing tests. The tribofilm thickness ranged from 75 nm at high humidity to 175 nm at low humidity [62]. Notably, the level of humidity did not appear to affect the time in which tribofilm thickness reached a steady state as all conditions maximized film thickness around 30 minutes of rubbing time. The influence of water within a tribosystem negatively impacts the effectiveness of the tribofilm which was shown by Soltanahmadi et al [50]. Using a modified MPR, similar to the device used in the present study, the researchers provided evidence that micropitting surface area and

abrasive wear increased with the amount of water present the lubricant [50]. The variance in tribofilm development due to environmental and operating conditions indicate close attention must be paid to the design of running-in with respect to tribofilms. Consideration must also be paid to the material and microstructure of the steel used because variations in the composition could contribute to the uneven tribofilm coverage.

The microstructure of hardened steels like those used in gears and bearings contain an inhomogeneous mix of different steel phases and levels of retained austenite and residual carbides. Investigators have shown the patches of tribofilm develop in sizes similar in magnitude to that of residual carbides and retained austenite [63].

CHAPTER 3. THE EFFECT OF CONTACT PRESSURE AND SURFACE TEXTURE ON RUNNING-IN BEHAVIOR OF CASE CARBURIZED STEEL UNDER BOUNDARY LUBRICATION

Adapted from paper submitted to *Wear*

Jeremy J. Wagner, Alexander D. Jenson, and Sriram Sundararajan
Mechanical Engineering, Iowa State University, Ames, Iowa 50011, USA

* Corresponding author
srirams@iastate.edu

Abstract

Many engineering tests start with a run-in procedure, as it is commonly accepted that running-in at some fraction of the target load is beneficial due to a reduction in surface roughness. However, the choice of load and duration is often based on historical context or the experience and philosophies of the testing personnel. The objectives of this study were to (1) evaluate the effects of contact pressure and initial composite roughness on the surface evolution during the initial stage of testing, and (2) use this information to determine if there is an optimal load and time for the run-in portion of a test. These tests were conducted with a disc-type machine using carburized steel specimens with a circumferential lay direction and oil with anti-wear additives under specific conditions of slide-to-roll ratio, entraining velocity, oil spin-off temperature, and oil/additive package. The specimen surface was inspected using non-contact profilometery every minute for the first 10 minutes of testing, with a subsequently increasing inspection interval for a total of 150 minutes. The data demonstrate that the surface roughness reduces within the first few minutes of testing and remains stable for a period, which is dependent on the pressure and initial composite roughness. Additionally, hardness measurements indicate that hardness gains are occurring during the test, but over a longer timeframe.

Introduction

Run-in, or break-in, is a term used to describe the initial changes to tribological bodies in contact. It is recognized by researchers that during run-in, the system adjusts to reach a steady-state condition between contact pressure, surface roughness, interface layer, and the establishment of an effective lubricating film at the interface. These adjustments may include surface conformity, oxide film formation, material transfer, lubricant reaction product, martensitic phase transformation, and subsurface microstructure reorientation [64]. The transition to the steady state condition is accompanied by complex irreversible phenomena that takes place in a thin surface layer [65].

Many engineering tests start with a run-in procedure, as it is commonly accepted that running-in at some fraction of the target load is beneficial. However, there are different philosophies regarding the load (e.g. 20% - 80%) and time (e.g. 75,000 – 600,000 cycles) used for the run-in portion of the test.

Most studies related to investigating the run-in phenomena have focused on understanding the effect of the entire test duration. Few studies have aimed to quantify and understand the evolution of the interface during the run-in process. Andersson [31] studied run-in of spur gears and found that the running-in period corresponded to less than 300,000 revolutions. Miller [66] studied run-in of cylindrical roller bearings and found that testing demonstrated dramatic changes in surface texture during the initial stages of testing for both moderate (1.48) and low (0.04) levels of λ. Miller also showed that components with a lower initial surface finish (honed), had a more pronounced initial drop in surface texture than components with a higher initial surface finish (ground). Akbarzadeh et al [67] saw a significant reduction in surface finish in their testing of discs at the first inspection interval of 10 minutes. Clarke et al [36] studied the surface evolution of axially ground discs, looking at the effect of hardness differential on run-in. Their work showed that run-in is a rapid process, happening in minutes. Sosa et al [10] studied the run-in of spur gears at two loads (0.9 and 1.7 GPa). Their work included 10 tests, one of which was stopped intermittently to evaluate the evolution of

the surface texture. Their intermittent evaluation showed that run-in of the surface occurred in 44 cycles at the higher load.

The objective of this study was to evaluate the effects of contact pressure and initial composite surface roughness on the evolution of surface texture and hardness during the initial stage of testing for a specific combination of slide-to-roll ratio (SRR), entraining velocity, oil spin-off temperature, and oil/additive package. It is recognized that if a tribofilm is generated during run-in, it will influence the surface evolution, and this effect could be different for different additive packages. However, the results in this study cover the applications of interest (gears and rolling element bearings in off-road equipment). Additionally, the goal is to use this information to determine if there is an optimal load and time for the run-in portion of a test.

Experimental Methods and Equipment

Sample Testing

The tests were run using the Micro Pitting Rig (MPR) from PCS Instruments (78 Stanley Gardens, London W3 7SZ, United Kingdom). The MPR, shown in *Figure 3a*, is a disc-type test machine with a test chamber as shown in *Figure 3b*. The central disc, called the roller, is the test specimen; the three outer discs, called the rings, are the counterfaces or load elements. This configuration enables three contact cycles per revolution of the test specimen. The MPR is computer controlled, and the speed of the roller and rings are controlled independently to allow for any combination of rolling and sliding. The MPR has a dip lubrication system, with the oil level 27.8 millimeters below the roller center, and it has an oil volume of 150 milliliters. The system has a heating/cooling unit that maintains the oil at the desired temperature. *Figure 3c* shows the details for a crowned roller, which was used for the tests in this study. A chamfered roller is also available as an option.

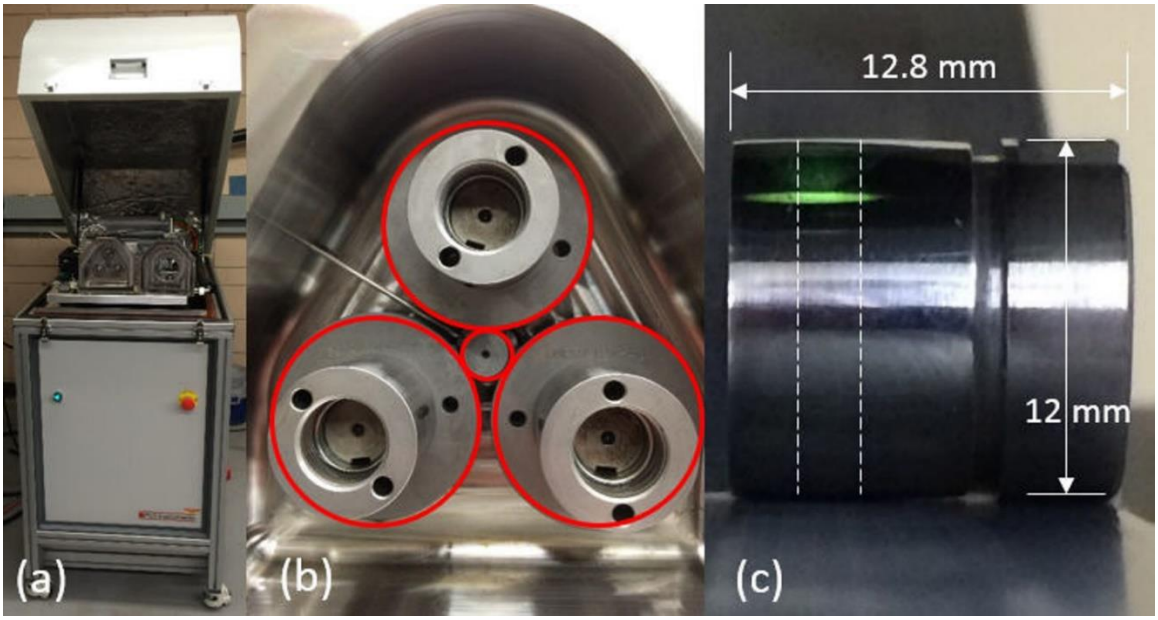

Figure 3. (a) Micro Pitting Rig (MPR) used in this study, (b) test chamber, and (c) roller. The roller is the test specimen and experiences three contact cycles per revolution. The approximate contact zone during testing is indicated by the dashed lines.

Eight tests were completed representing four test conditions with a replicate at each condition (*Table 3*). The total test time was 150 minutes, which is equivalent to 109,669 contact cycles. For all the tests, the slide-to-roll ratio was 20%, the entraining velocity was 0.17 m/s, and the oil spin-off temperature was 80 °C. These conditions result in boundary lubrication for all test conditions shown in *Table 3*. All the rollers had the same roughness specification, while the rings had two different values of initial roughness to achieve the two levels of composite roughness. Roughness specifications for the roller and rings are listed in *Table 5*.

Table 3. Test conditions (a replicate was run at each condition).

Test	Pressure[a] (GPa)	Composite Roughness[b], Ra, (µm)	Composite Roughness[c], Rq, (µm)	Lambda Ratio[d, e]
A	1	0.20	0.21, 0.23	0.096, 0.086
B	2		0.30, 0.33	0.056, 0.052
C	1	0.47	0.69, 0.67	0.029, 0.030
D	2		0.65, 0.65	0.026, 0.026

[a] max Hertzian pressure
[b] calculated from manufacturer's specifications
[c] based on initial, measured surface roughness, one value for each replicate
[d] based on Hamrock-Dowson minimum film thickness

The slide-to-roll ratio (SRR) is defined as:

$$SRR\ (\%) = \frac{U_1 - U_2}{{}^1/_2(U_1 + U_2)} \tag{5}$$

Where U_1 is the ring speed and U_2 is the roller speed. With this convention, a positive SRR indicates the roller speed is slower than the ring speed.

Each test was divided into 25 segments, and the length of the segments varied from 1 to 15 minutes as shown in *Table 4*. At the end of each segment, the test was stopped, and the surface texture was measured as described in Section 2.3. The roller was then inserted back into the MPR, and the test was continued. Each test segment was preceded by a warmup period of approximately 30 minutes to stabilize the oil spin-off temperature at 80 °C. During the warmup, there was no applied load and no sliding (SRR = 0) with an entrainment speed of 1 m/s.

Table 4. Test segments. Surface texture was measured at the end of each segment.

Test Time (min)	Segment Time (min)
0 - 10	1
10 – 20	2
20 – 30	5
30 - 150	15

Materials

All test specimens were 16MnCr5 steel that was carburized and finish ground with a circumferential surface texture lay direction. The manufacturer's specifications (PCS Instruments) for surface roughness and hardness for individual parts are listed in *Table 5*. The initial composite roughness was varied by using a smooth or rough ring. The microgeometry of the rollers included a 76.2-mm crown, while the rings were flat.

Table 5. Roller and ring surface roughness and hardness specifications (per manufacturer).

Part	Roughness, Ra (µm)	Hardness (HV)	Case Depth (mm)
Roller (specimen)	0.15 ± 0.05	680 ± 20	0.9 min
Ring (smooth)	0.125 ± 0.025	750 ± 20	0.9 min
Ring (rough)	0.45 ± 0.05	750 ± 20	0.75 - 1

The oil used in this study was an API Group II base oil with ZDDP anti-wear and other additives. One of the additional additives was a viscosity index (VI) improver, so the oil was sheared prior to testing by running it through a piston pump for 48 hours. Shearing the oil prior to testing ensures that changes in viscosity as a result of shearing do not affect the test. The kinematic viscosity of the sheared oil was 50.51 – 51.44 cSt at 40 °C and 7.56 – 7.81 cSt at 100 °C.

Profilometry

The roller surface texture was inspected using a Zygo NewView 7100 optical profiler at six equally spaced circumferential locations, and the texture parameters were evaluated and reported as an average of these six measurements. The data was obtained using a 20X objective resulting in a scan area of 0.47 mm (axial direction) by 0.35 mm (circumferential direction). Ten standard surface texture parameters were evaluated from these measurements to determine the best indicator of run-in. These included: average roughness (Ra), root mean square roughness (Rq), ten-point height (Rz), kurtosis (Rku), skewness (Rsk), and the material ratio parameters (Rk, Rpk, Rvk, MR1, MR2).

The cylinder removal feature was applied to the raw data in the Zygo to remove the effects of the roller curvature on the surface texture. Additionally, the raw data sets were normalized to account for variation in initial roughness of the test specimens. This was done by simply dividing each measured parameter value by the baseline (initial) measurement prior to testing.

Hardness Testing

Hardness testing was performed using a LECO LM247AT Microhardness Tester & Amh43 Software. The Amh43 program controlled the position of the specimen stage and captured images of indents made on the roller specimens.

Indents were made using a Vickers diamond tip with a face angle of 136° which was force-controlled with a 13-second dwell time. Hardness measurements were taken at positions around the circumference of the roller, every 60°, for a total of six different positions. At each position, three indents were made using a 500-gf load and another three were made using a 50-gf load. The indents were spaced axially along the roller per the ASTM E384 standard (spacing was at least 2.5*diagonal length between indents). These indents were made both inside and outside the contact zone of each roller to establish relative hardness between the worn and unworn areas at each position.

Using the Amh43 Software, indents were first measured automatically to determine general diagonal length, then refined by manually selecting indent corners (Amh43 software user interface was easily distracted by geometry, especially at a 50-gf load where resolution made selecting indent corners difficult). With the indent corners selected, the two diagonals of the indent were recorded to calculate an average diagonal length, which was used to calculate the Vickers hardness (VDH) as per Fischer-Cripps [68]. Estimation of the indentation depths, based on the geometry of the tip and the average of the diagonals, yielded values of approximately 1.4 µm for the 50-gf load and approximately 4.9 µm at the 500-gf load.

Results and Discussion

Ra and Rz were chosen from the ten surface texture parameters evaluated as the optimal indicators of run-in. While several other parameters showed similar trends, Ra was chosen because it is a familiar parameter to many engineers, and Rz was chosen since one would expect the value of this parameter to reduce over time as asperity peaks deform and/or wear, and the peak to valley dimension is reduced. *Figure 4, Figure 5, Figure 7 and Figure 8* show the evolution of the Ra and Rz parameters for the various test conditions. These figures can be compared horizontally to look at the effect of pressure on run-in and vertically to compare the effect of initial composite roughness on run-in. In these figures, the decimal in the test name indicates the replicate number for a given test condition (A-D as described above in *Table 6*).

Figure 4 and *Figure 5* show Ra and Rz for the complete test duration. Recall that the data are reported normalized to the initial baseline values, allowing for easier comparison. The average baseline Ra values for the rollers varied between 0.03 µm and 0.11 µm, while the average baseline Rz values for the rollers varied between 0.40 µm and 1.96 µm. For all tests, both Ra and Rz reduce significantly immediately, followed by a period of stabilization where the surface texture parameters settle into a steady state value. Rz showed the same overall trend as Ra, but it was more sensitive to grooves (both depth and quantity), which tended to obscure the data. This is especially noticeable in the Rz plot for A.1 where grooves caused an increase between 10 and 45 minutes that was not representative of the entire surface.

The main difference in run-in under different conditions is what happens after the stabilization period. At the lower pressure of 1 GPa, the roughness remained low throughout the test, regardless of initial composite roughness. At the higher pressure of 2 GPa, the roughness increased and was further affected by initial composite roughness. At low composite roughness (0.20 µm), the test specimen roughness increased at 30 minutes, but then remained relatively constant; at high composite roughness (0.47 µm), the test specimen roughness also increased and continued to increase throughout the test. The increase in test specimen roughness in this case can be attributed to the

occurrence of surface damage. Representative images of the surface progression for one sample from each test condition are shown in *Figure 6*. In this figure, the majority of the machining marks are gone after 5 minutes for all the tests. Tests B and D, which were run at the higher pressure, have signs of damage at 30 minutes, as noted by the arrows. This damage appears relatively the same for test B between 30 and 120 minutes, but it noticeably increases for test D between 30 and 120 minutes. This helps explain the difference in the behavior of the Ra trends for tests B and D.

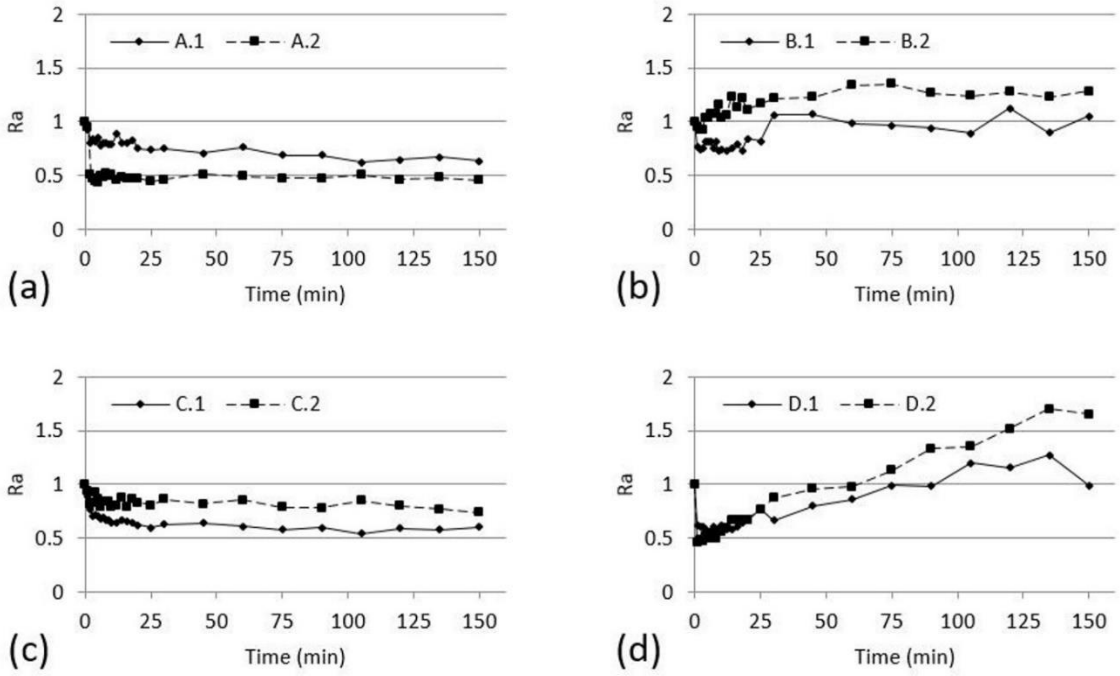

Figure 4. Evolution of normalized Ra for complete test duration for (a) test A replicates, (b) test B replicates, (c) test C replicates, and (d) test D replicates.

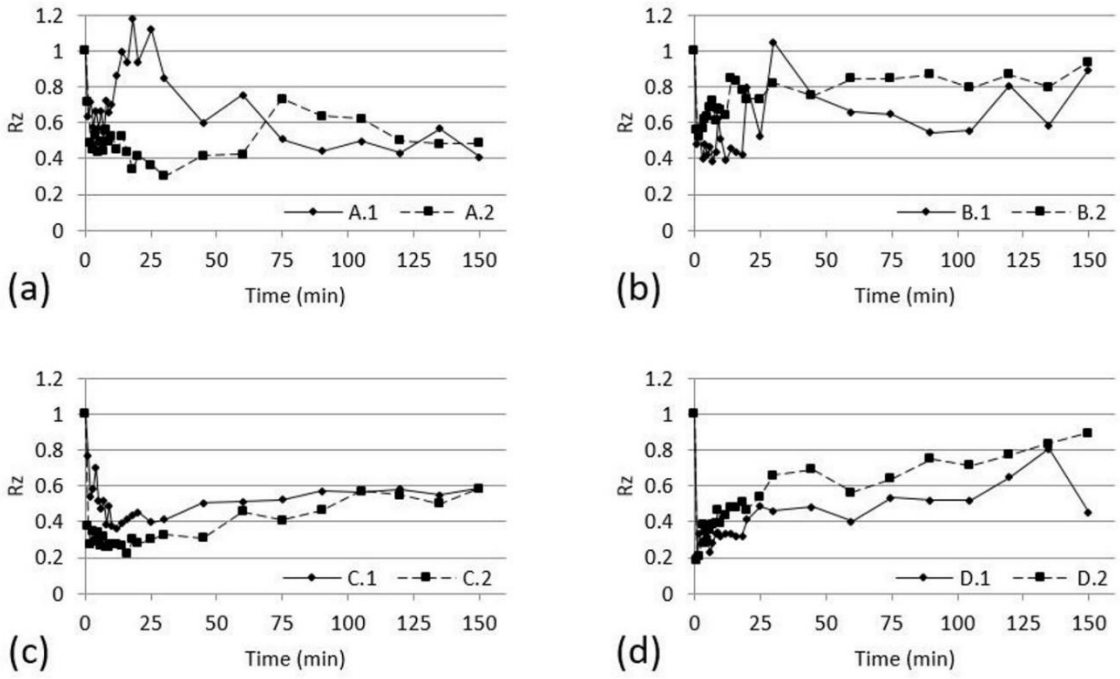

Figure 5. Evolution of normalized Rz for complete test duration for (a) test A replicates, (b) test B replicates, (c) test C replicates, and (d) test D replicates.

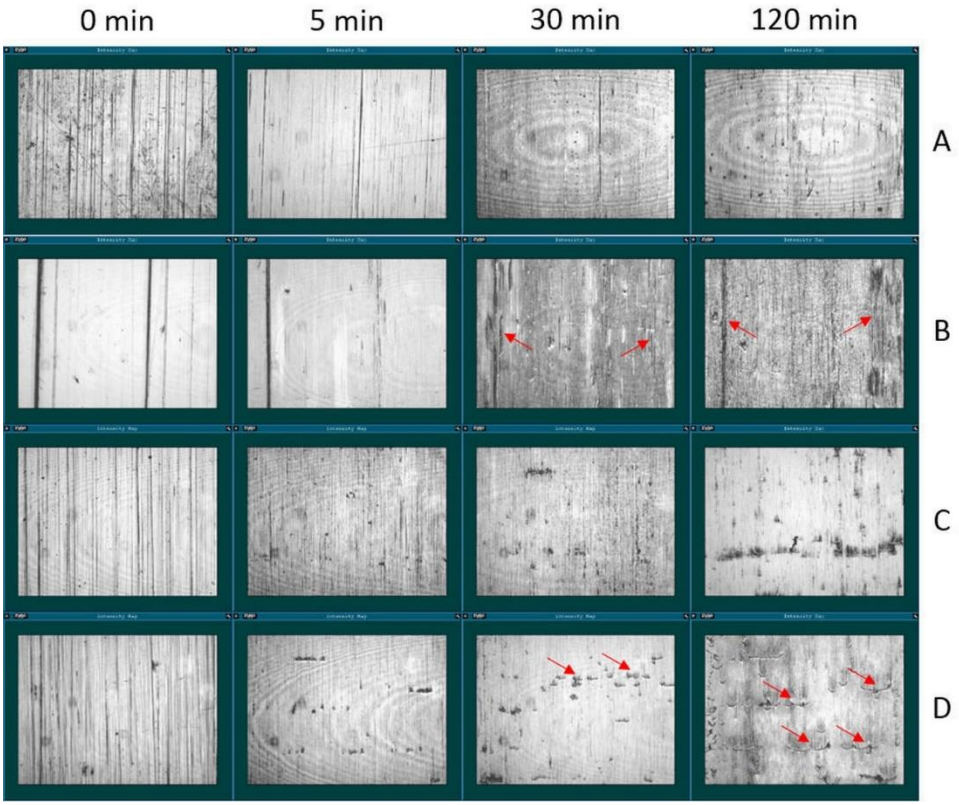

Figure 6. Illustrative surface images of the roller at 0, 5, 30, and 120 minutes for the various test conditions.

Figure 7 and *Figure 8* show Ra and Rz for only the first 30 minutes of testing, and emphasize how quickly the surface finish shows a significant reduction, regardless of pressure or initial composite surface roughness.

Figure 7 and *Figure 8* also illustrate the differences in the amount of reduction in Ra and Rz for the various test conditions. In general, a higher initial composite roughness seems more beneficial to reduce the roughness of the specimen. In comparison, increasing the contact pressure does not seem to provide as much of an improvement. The difference in the amount of initial roughness improvement can be attributed to the difference in initial roughness, especially the Rz values. *Table 6* lists the average measured initial Ra and Rz values for the rollers for each of the tests. It appears that in cases where the replicates had significant differences in initial Rz (e.g. conditions A and B), there is more scatter in the amount of reduction in the roughness during the run-in. The samples with the higher initial roughness show a greater reduction than the samples with the lower initial roughness, which suggests that the taller asperities get smoothened out more.

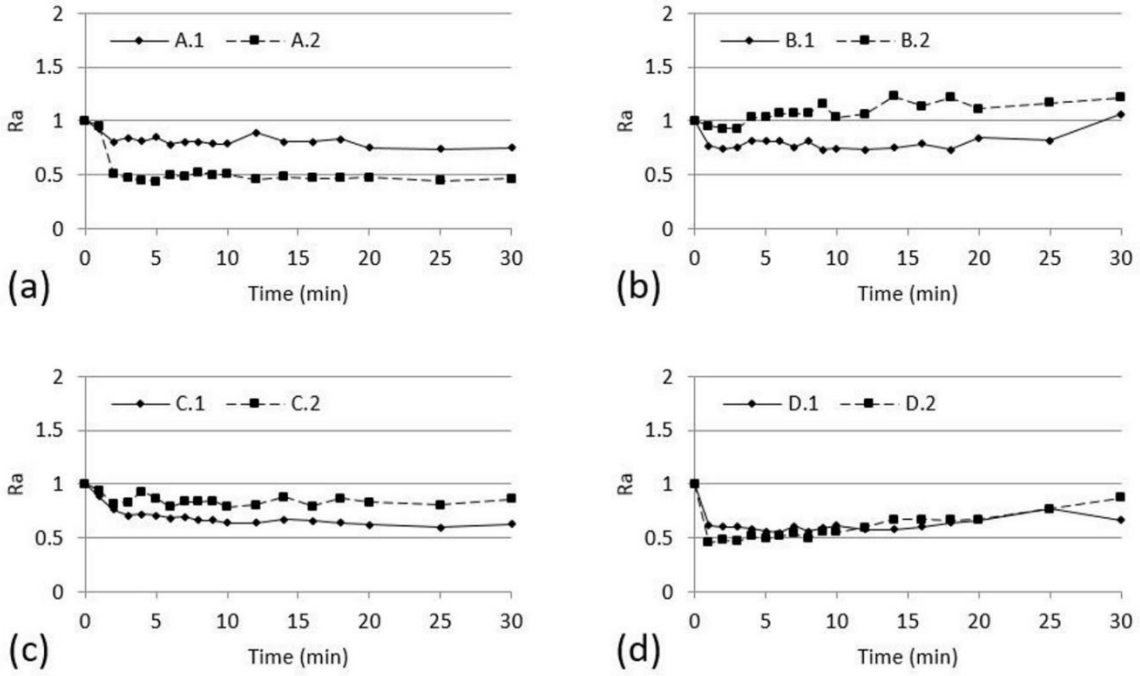

Figure 7. Evolution of normalized Ra, first 30 minutes of test, for complete test duration for (a) test A replicates, (b) test B replicates, (c) test C replicates, and (d) test D replicates.

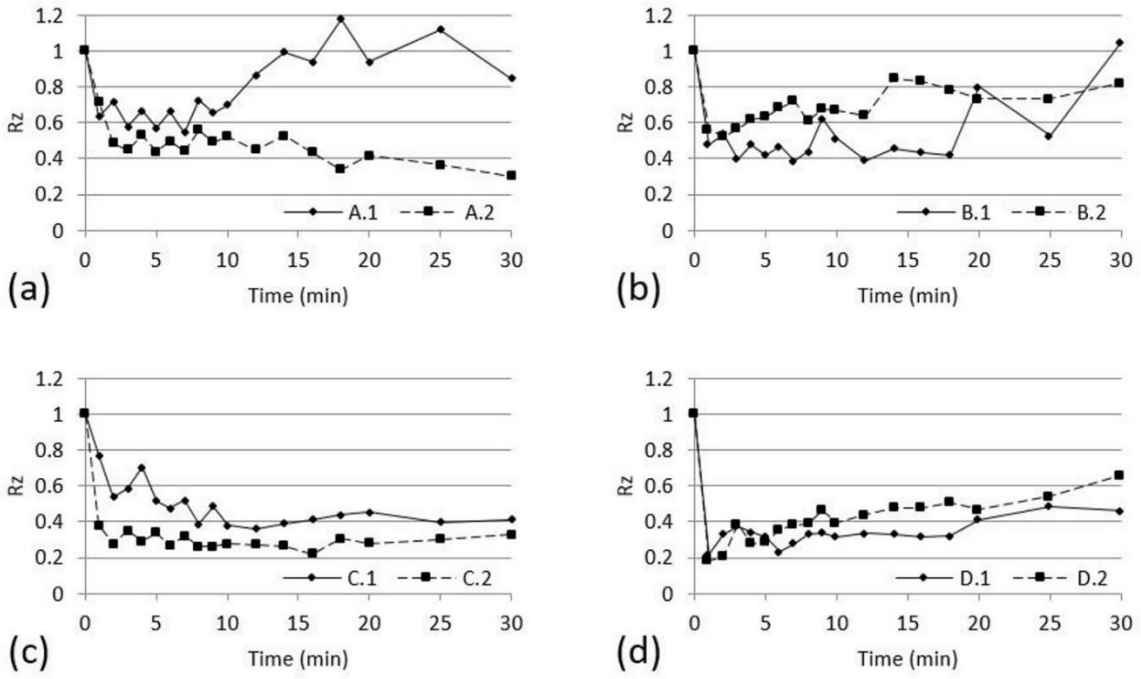

Figure 8. Evolution of normalized Rz, first 30 minutes of test, for complete test duration for (a) test A replicates, (b) test B replicates, (c) test C replicates, and (d) test D replicates.

Table 6. Average measured initial roughness.

Test	Ra (µm)	Rz (µm)
A.1	0.03	0.40
A.2	0.08	1.57
B.1	0.08	0.85
B.2	0.10	1.96
C.1	0.11	1.57
C.2	0.05	1.21
D.1	0.04	0.97
D.2	0.05	0.96

Additionally, autocorrelation length of the surface is being evaluated to determine if run-in influences the evolution of the spatial characteristics of the surface texture. The initial results indicate that the initial composite roughness might have an influence on the evolution of the autocorrelation length.

Another indicator of run-in is the evolution of friction behavior. Friction data is calculated by the MPR using the measured torque and force. The friction evolution data is shown in *Figure 9*, and it is noted that the friction had the same immediate reduction as the surface roughness parameters. The initial values were in the range of 0.12 – 0.15, settling in around 0.11 or lower within 5 minutes of running, which is the same timeframe that it takes the surface roughness to stabilize.

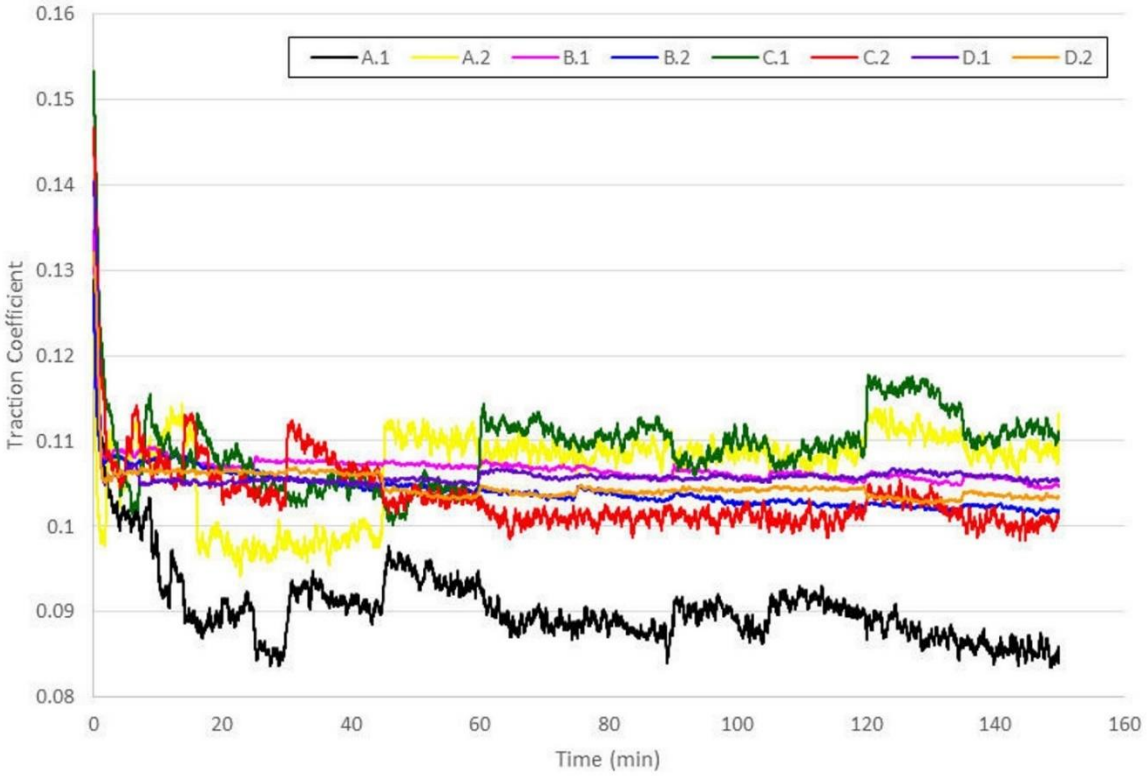

Figure 9. Evolution of friction coefficient for all the samples for the duration of the run-in tests.

Weight loss measurements and roller diameter measurements suggested no significant change, and profilometry also did not reveal discernable wear depth for the contact zone. This indicates that any wear during run-in is at the asperity level and via localized damage as shown in *Figure 6*. It should be noted that the surface roughness parameters and friction behavior can be influenced by the formation of a tribofilm during the run-in process. Tribofilms have been reported to form in the presence of ZDDP additives in the oil [69–71].

Figure 10 shows the relative hardness (hardness inside the contact zone minus the hardness outside the contact zone) for the various test conditions. The data indicated the surface underwent hardness gains under all the test conditions, but most notably under the higher initial composite roughness and lower contact pressure condition (test condition C). Hardness gains during wear under low pressure have also been reported for 3140 steel [72].

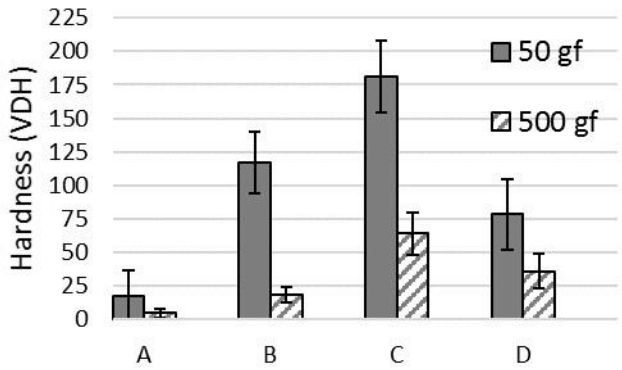

Figure 10. Relative hardness (hardness inside contact zone minus hardness outside contact zone) per test conditions A-D. Average of 36 values are shown along with a 90% confidence interval.

An analysis of variance of the data indicated a significant difference between the hardness inside the contact zone to that of the hardness outside the contact zone for test conditions B-D. The hardness gains were more pronounced near the surface as evidenced by the gains in hardness at 50 gf which corresponded to depths of 1.4 µm as compared to the gains at 500 gf, which were at depths of 4.9 µm.

Hardness increases near the surface could be attributed to tribochemical surface films formed during testing. Literature suggests the ZDDP anti-wear additive in the oil used can form a tribofilm around 100 - 200 nm thick [69–71], and that these tribofilms can exhibit slight increases in hardness with sliding time [73]. Thus, the hardness gains observed at the lower indentation load of 50 gf, which reached an average depth of 1.4 µm, can conceivably be influenced by any tribofilms that may have formed during run-in. Hardness gains can also be attributed to work hardening as evident by the relative hardness gains seen at the higher indentation loads of 500 gf, which reached an average

depth of 4.9 µm, and which far exceed the estimated tribofilm thicknesses reported in the literature.

The data suggest that at low levels of composite roughness (0.20 µm), increasing the applied load (1 GPa to 2 GPa) results in higher levels of hardness gains. Interestingly, at a higher composite roughness (0.47 µm), an increase in applied load did not provide a gain in hardness. Rather, it appeared to suppress it.

The observations on hardness gains are for the entire test duration (150 minutes). Current work is aimed at evaluating the evolution of the hardness, including formation of any tribofilms. Initial data suggests the hardness gains may not be occurring within the timeframe in which the surface texture stabilizes.

Summary and Conclusions

Testing was conducted for approximately 110,000 cycles to evaluate the effects of contact pressure and initial surface roughness on the evolution of surface texture, friction, and hardness during the early stage of testing for a specific combination of slide-to-roll ratio, entraining velocity, oil spin-off temperature, and oil/additive package. The surface roughness and the friction data demonstrate that run-in of the surface occurs almost immediately (within 5 minutes), regardless of the pressure or initial composite surface roughness. Neither the pressure (1 vs. 2 GPa) nor the initial composite roughness (0.20 µm vs. 0.47 µm, spec) had a significant effect on the initial reduction in surface texture values. However, it did influence how the surface texture evolved after the initial reduction. A combination of higher pressure and higher initial composite roughness results in early damage to the surface that does not stabilize within the test timeframe. This is illustrated in *Figure 4d* and *Figure 6*.

Comparing the results of the present study to the work of Clarke et al [36] indicates that surface texture lay direction is not a dominant factor in run-in. Clarke used discs with an axial lay direction, and discs with a circumferential lay direction were used here. In both cases, the surface roughness reduced significantly immediately.

The samples in this study showed evidence of hardness gains in the contact zone at the end of all the tests. The increase in hardness could be attributed to a combination of the formation of tribofilms as well as work hardening. The increase in hardness was influenced by both the applied pressure and initial composite roughness. The largest gains were at the condition of low pressure and higher initial composite roughness. Testing is currently in process to determine the timeframe in which this transition occurs.

If the test objective is to make the surface smoother, the results indicate that this happens in minutes. If the objective is to improve material properties, initial results indicate a longer test time may be needed.

CHAPTER 4. THE EVOLUTION OF HARDNESS AND TRIBOFILM GROWTH DURING RUNNING-IN OF CASE CARBURIZED STEEL UNDER BOUNDARY LUBRICATION

Adapted from paper submitted to *Wear*

*Alexander D. Jenson, Sougata Roy, and Sriram Sundararajan**
Department of Mechanical Engineering, Iowa State University, Ames IA 50011, USA

**corresponding author*
srirams@iastate.edu

Abstract

Many newly manufactured components are subject to a run-in procedure. It is commonly accepted that performing running-in at a fraction of the target load is beneficial due to a reduction in the surface roughness of the interacting surfaces. During this process, many changes take place within the surface layer including transformations in surface roughness, chemistry, and microstructure. These transformations can contribute to changes in the surface mechanical behavior of the components. The objective of this study was to understand how the surface hardness of 16MnCr5 bearing steel evolved during running-in and how varying contact pressure and initial composite roughness affected this evolution. The evolution of the tribofilm formed by zinc dialkyl dithiophosphate (ZDDP) and how it contributed to the measured hardness was also analyzed. The results indicated a higher initial composite roughness led to greater gains in hardness as compared to higher contact pressure during the running-in process. Tribofilm growth appeared to have little to no significant effect on the measured surface hardness increase during running-in and the primary contributor to the observed hardness increase was work hardening. The results of this study can inform engineers and manufacturers in their efforts to optimize running-in procedures, thereby increasing the efficiency and durability of their service components.

Introduction

Running-in is the initial wear and plastic deformation of interacting surfaces, starting with the conditions after manufacturing. It is understood that run-in is achieved when a steady-state of friction or mild wear is reached. The transformation of wear and friction are characterized by changes in the thin surface layer's conformity, oxide film formation, material transfer, lubricant reaction product, martensitic phase transformation, and subsurface microstructure reorientation [25]. However, there is a gap in understanding all the changes which occur during in the initial phases of running-in which was identified by Blau [15]. Much of the research performed still has not fully characterized the details of run-in and yet run-in is often utilized as a starting procedure for tribotests [8,9,6]. If engineers fully understood the running-in process it would be invaluable in enhancing the operation and extending the life of tribosystems.

One aspect of running-in which has been studied extensively is the change in surface roughness. Abbott and Firestone's work initially sparked the drive to understand the topography changes of surfaces during run-in when they characterized the asperities which come into contact with one another [26]. Anderson determined running-in occurred at around 300,000 cycles when observing the wear of asperities and the surface roughness [31]. Research by Martins et al. showed a significant smoothening of asperities occurred after 90,000 cycles under a low load [74]. Akbarzadeh and Khonsari indicated lowering the surface roughness in gears could improve the system [35]. Researchers who study the roughness during run-in use show transformations in Ra, Rmax, Rku, Rq, and Rsk [75,76].

Instead of focusing solely on the wear aspects of running-in, Berthe et al. analyzed the surface mechanics of the asperities during running-in and showed the plastic deformation stabilized after ten cycles [16]. Zwirlein and Schlicht observed compressive residual stresses could be generated through cyclic stresses and strengthen the subsurface [77]. Burbank and Woydt sought to utilize the running-in as a controlled work hardening and observed increased operational lifetimes for different steel types [17].

Zinc dialkyl dithiophosphate (ZDDP) is an anti-wear agent present in most automotive lubricants blends and reduces wear and scuffing between metal surfaces by forming a boundary film (tribofilm) [78,79]. A study by Aktary et al. indicated tribofilms develop rapidly (5 minutes) after rubbing tests on 5210 steel [52]. Parsaeian et al. measured the tribofilm growth under varied humidity conditions and showed, for all conditions, the tribofilms reached a maximum thickness between 20-30 minutes of rolling-sliding contact [62]. Work by Kalin et al. showed the ZDDP tribofilm hardness properties evolved as a function of test duration and had measurable hardness after 25 minutes [73].

Previous work by Wagner et al. paralleled this immediacy of run-in [80]. Wagner et al. also showed evidence of hardness gains within the contact region following approximately 110,000 cycles. It was shown that run-in occurs at a relatively low number of contact cycles and hardness gains are present in this time frame as well, and it was proposed work hardening develops early on within the same number of cycles.

The purpose of this study was to characterize the evolution of hardness during the early stages of running-in of 16MnCr5 steel for a specific combination of slide-to-roll ratio (SRR), entraining velocity, oil spin-off temperature, and oil/additive package. The effect of contact pressure and initial composite surface roughness on the hardness evolution were also studied. Tribofilms can develop on steel surfaces during rolling-sliding contact, so energy-dispersive X-ray spectroscopy (EDS) point analysis was used to detect the presence of a tribofilm within the wear track region. Since tribofilms might influence the measured hardness, an attempt to characterize the hardness gains as a combination of work hardening and the influence of the presence of tribofilms was also explored. The results of this study cover the application of interest (gears and rolling element bearings in off-road equipment), so the effect could be different for different conditions.

Experimental Methods and Equipment

Run-In Testing

Tests performed in this study were run using a Micro Pitting Rig (MPR) by PCS Instruments (*Figure 11a*). The MPR is a computer controlled disc-on-disc contact instrument in which three 'counter face' rings of equal diameter positioned apart with a smaller diameter roller (sample) located in the center (*Figure 11b*). With the roller in contact with the three rings, it experiences three contact cycles per revolution. The speeds of the rings and rollers can be controlled independently, allowing for different combinations of rolling and sliding contact. The MPR utilizes a dip lubrication system, with the oil level 27.8 millimeters below the center of the roller and a volume of 150 milliliters. The unit is also temperature controlled to maintain the desired operating temperature. A crowned roller was used for the tests performed in this study and its dimensions and approximate contact zone can be seen in *Figure 11c*.

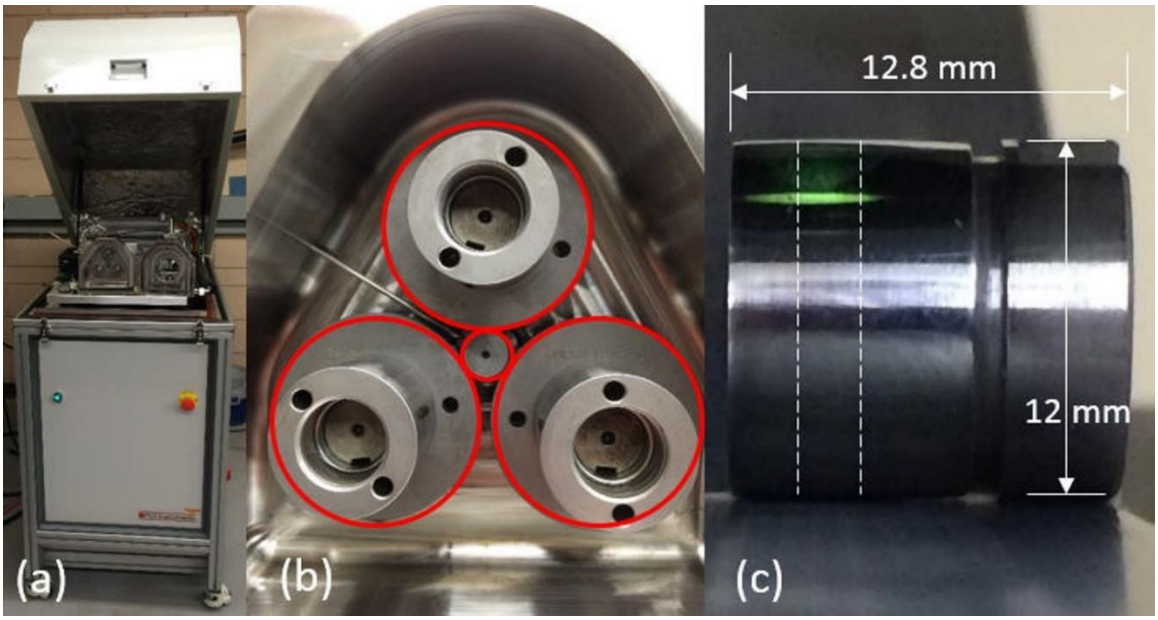

Figure 11. (a) Micro Pitting Rig (MPR) used in this study, (b) test chamber showing the central roller (sample) and three rings, and (c) dimensions of the roller. Dashed lines indicate approximate contact zone.

Tests were conducted under two different contact pressures and two different initial composite roughness (conditions A-D) as indicated in *Table 7.* From the previous study by Wagner et al., test condition A showed insignificant hardness gains compared to conditions B-D [80]. When current tests yielded similar results under condition A, it was decided to focus on the other three conditions. One test was run under condition A, two tests under conditions B and D, and one test under condition E (*Table 7*). Tests under conditions A-D were performed using an API group II base oil with ZDDP additives. The test under condition E was performed using an API group II base oil without ZDDP additives. The film thickness ratio (λ) was calculated using the Hamrock-Dowson minimum film thickness and measured initial composite roughness (Rq) to verify tests were run under boundary lubrication. However, for condition E, the exact physicochemical properties of the group II base oil without ZDDP additives were not known, so a range for the film thickness ratio was reported (*Table 7*) based on properties found from literature [81]. Based on the variance in this range, the authors assumed condition E operated under a boundary lubrication condition consistent with the other tests.

Table 7. Test samples and contact load conditions.

Test	Pressure[a] (GPa)	Composite Roughness[b], Ra (µm)	Composite Roughness[c], Rq, (µm)	Lambda Ratio[d] (λ)	Lubricant (API Group II Base Oil)
A	1	0.20	0.17	0.118	*with* ZDDP additives
B	2		0.18, 0.18	0.095, 0.094	
C	1	0.47	0.53, 0.54, 0.52	0.038, 0.037, 0.039	
D	2		0.53, 0.54	0.032, 0.032	
E	1		0.51	0.017-0.037	*without* ZDDP additives

[a] Max Hertzian pressure
[b] Calculated per manufacturer's specifications
[c] Calculated per measured initial surface roughness
[d] Based on Hamrock-Dowson minimum film thickness

The other parameters held constant for every test are shown in *Table 8*. Slide-Roll ratio (SRR) is define by *Equation 1*:

$$SRR\ (\%) = \frac{U_1 - U_2}{{}^1/_2(U_1 + U_2)} \quad (6)$$

where U_1 is the ring speed and U_2 is the roller speed. All of the rollers had the same initial surface roughness (as per manufacturer) at 0.15 ± 0.05 µm, while the rings were either smooth or rough, 0.125 ± 0.025 or 0.45 ± 0.05 respectively, to achieve the two levels of initial composite roughness (Ra). Measured initial composite roughness values (Rq) are found in Table 7.

Table 8. MPR conditions used for all tests. Parameters resulted in boundary lubrication for all conditions.

Parameter	Value
Time	150 minutes
Contact Cycles	109,669 cycles
SRR (Eq. 6)	20%
Entraining Velocity	0.17 m/s
Spin-off Temperature[a]	80 °C

[a] Spin-off Temperature was measured by a temperature probe inserted into the test chamber with the tip of the probe placed close to the contact region

Tests were divided into five, 30-minute segments as outlined in *Table 9*. At the end of every segment, the test was stopped, the roller was removed and the surface texture and hardness were measured as described in Sections 2.3 and 2.4 respectively. Following the measurements, the roller was inserted back into the MPR and the test was continued. A warmup phase of about 30 minutes was run at the start of each segment to stabilize the oil spin-off temperature at 80 °C before running-in continued. No load nor sliding (SRR = 0) was applied during the warm up phase and the entrainment speed was held at 1 m/s. A measurement interval at 15 minutes (10,967 contact cycles) was added for the two tests run for the tribofilm film analysis.

Table 9. Test intervals. Surface texture and hardness were measured at the end of each segment.

Test Time (min)	Contact Cycles
0 - 30	21,934
30 - 60	43,868
60 - 90	65,801
90 - 120	87,735
120 - 150	109,669

Materials

All test rollers were made from 16MnCr5 steel, case carburized to an approximant depth of 9 mm, and finish ground with a circumferential surface texture lay direction. Carbon content in the steel was 14% to 19%. The initial composite roughness, as listed in *Table 7*. was varied by using a smooth or rough ring. The microgeometry of the rollers included a 76.2-mm crown, while the rings were flat.

The lubricating oil used in this study was an API Group II base oil with ZDDP anti-wear and other additives. One of the additional additives was a viscosity index (VI) improver, so the oil was sheared prior to testing by running it through a piston pump for 48 hours. Shearing the oil prior to testing ensures that changes in viscosity because of shearing does not affect the test. The kinematic viscosity of the sheared oil was 50.51 – 51.44 cSt at 40 °C and 7.56 – 7.81 cSt at 100 °C.

Profilometry

The roller surface texture was inspected using a Zygo NewView 7100 optical profiler at three equally spaced circumferential locations, and surface roughness parameters were evaluated and reported as an average of these three measurements. The data was obtained using a 20X objective resulting in a scan area of 0.47 mm (axial direction) by 0.35 mm (circumferential direction). The cylinder removal feature was applied to the raw data in the Zygo to remove the effects of the roller curvature on the surface texture prior to analysis of surface roughness. Additionally, the raw data sets

were normalized to account for variation in the initial roughness of the test specimens. This was done by simply dividing each measured parameter value by the baseline (initial) measurement prior to testing.

Hardness Testing

Hardness testing was performed using a LECO LM247AT Microhardness Tester & Amh43 Software. The Amh43 program controlled the position of the specimen stage and captured images of indents made on the roller specimens.

Indents were made using a Vickers diamond tip with a face angle of 136° which was force-controlled with a 13-second dwell time. Hardness measurements were taken at positions around the circumference of the roller, every 120°, for a total of three different positions. At each position, three indents were made using a 500-gf load and additional three were made using a 50-gf load. Using the Amh43 Software, indents were first measured automatically to determine general diagonal length, then refined by manually selecting indent corners. With the indentation corners selected, the two diagonals of the indent were recorded to calculate an average diagonal length, d, which was used to calculate the Vickers hardness (HV) as follows for a given load, F (Eq. 7).

$$HV = \frac{2F\,sin\frac{136^\circ}{2}}{d^2} \qquad (6)$$

The indents were spaced axially along the roller per the ASTM E384 standard. These indents were made both inside (H_{in}) and outside (H_{out}) the contact zone of each roller. Results from the hardness measurements were normalized to account for variation in the initial hardness of the test specimens. This was done by taking the average hardness inside the wear zone for each time interval, t, and dividing it by the average hardness outside the wear zone from the entire test duration, $\overline{H}_{out}$. $\overline{H}_{out}$ was used as the baseline because this region was well outside the area which underwent running-in, and the hardness from this region, as expected, did not change much.

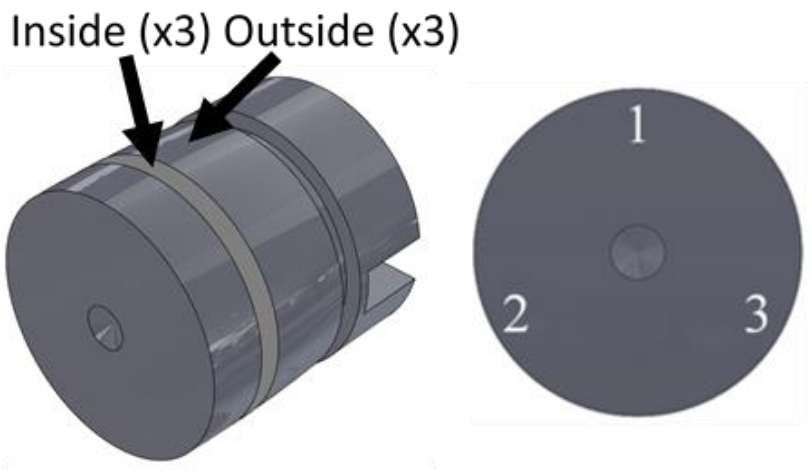

Figure 12. (Left) Locations for hardness measurements inside and outside wear track. (Right) Circumferential locations for hardness measurements.

Tribofilm Analysis

An FEI Quanta-250 Scanning Electron Microscope (FESEM) was used to obtain high-resolution images of wear tracks and an Oxford Aztec energy-dispersive x-ray analysis was used to perform point analysis of the wear track and adjacent regions for evidence of tribofilm formation. Backscattered images were analyzed for further tribofilm analysis with an accelerating voltage 8 kV and spot size 4.8 A.U. for all cases. Maintaining an acceleration voltage of 8 kV was optimal for collecting data from the near-surface region where tribofilms can potentially develop. Backscattered electron images were used to detect areas where low atomic number elements like those found in ZDDP-based tribofilms would appear darker than the high atomic number elements found in the base material.

Results and Discussion

Roughness Evolution

Figure 13 and *Figure 14* show the evolution of surface roughness parameters Ra and Rz, respectively, as a function of contact cycles, for the various test conditions. These figures can be compared horizontally to observe the effect of increasing contact pressure on run-in and vertically to compare the effect of increasing initial composite

roughness on run-in. The 90% confidence interval for these measurements was about 15-20%. The data shows that in all cases, the normalized parameters reduce quickly to almost 0.5 at approximately 20,000 contact cycles or about 30 minutes. A detailed analysis of the roughness evolution was the focus of a previous study by Wagner et al. [80]. The conditions which had lower contact pressure (B and C), show surface roughness stabilized after the first approximately 20,000 contact cycles. For the higher contact pressure conditions (C and D), surface roughness appeared to steadily increase after the initial drop after approximately 20,000 contact cycles. In general, increasing initial composite roughness seems more beneficial to reduce the roughness of the material during run-in as compared to an increase in contact pressure.

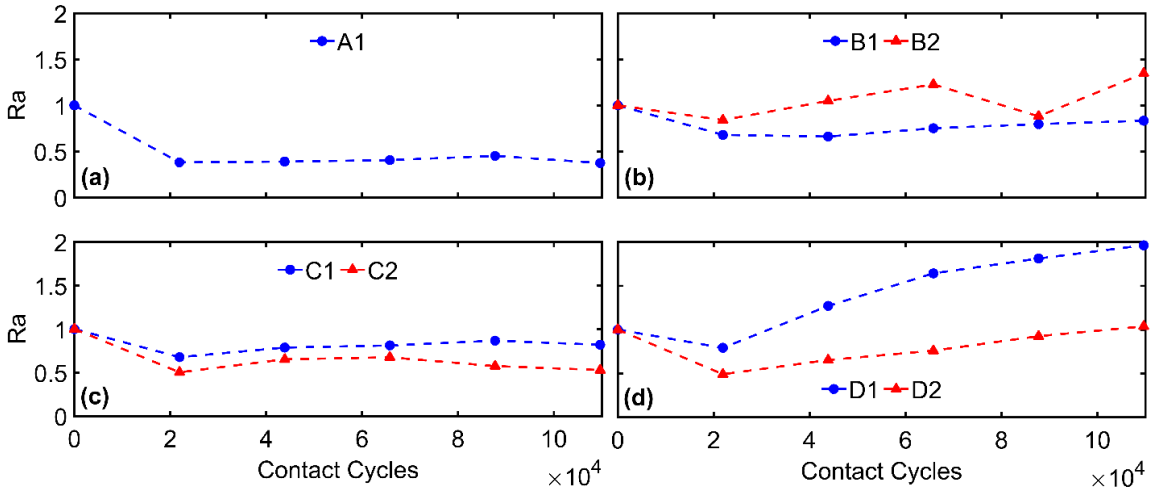

Figure 13. The normalized surface roughness (Ra) for conditions A, B, C, and D.

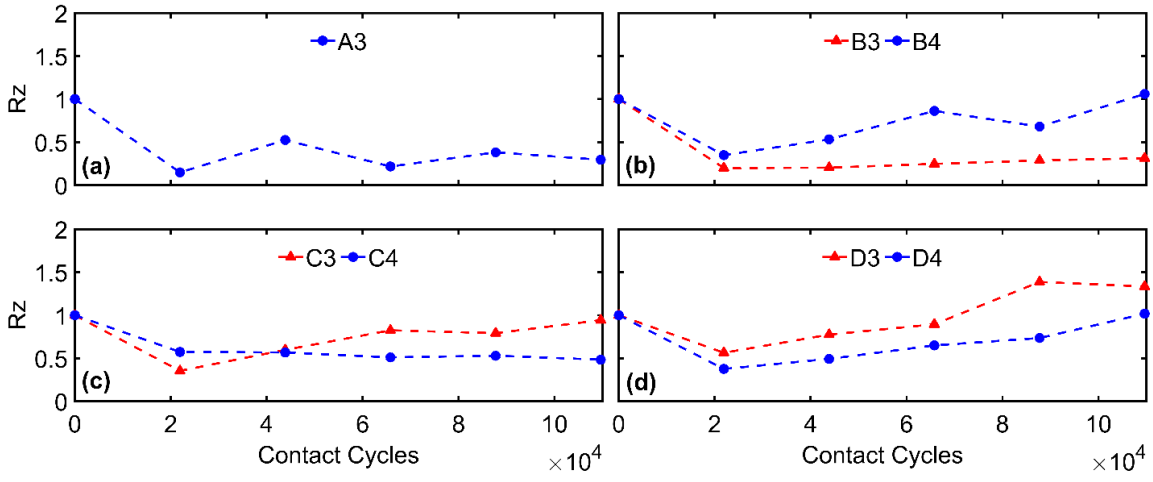

Figure 14. The normalized surface roughness (Rz) for conditions A, B, C, and D.

Hardness Evolution

Figure 15 shows the normalized hardness as a function of running-in contact cycles for the various test conditions. *Figure 15a* and *Figure 15b* show the hardness data collected using a 50-gf and 500-gf indenter load respectively. The data indicates the area inside the wear track experiences an increase in hardness, as compared to the unworn region, following run-in which is consistent with the previous study [80] and other work by Burbank and Woydt [17]. *Figure 15a* shows hardness gains range from minimal changes for condition A to about 20% for condition D, as measured with a 50-gf indenter load (corresponding to an indentation depth of about 1.4 µm). *Figure 15b* shows hardness gains are relatively lower as measured with a 500-gf indenter load (corresponding to an indentation depth of 4.8 µm), ranging from minimal hardness gains under condition A to about 8% under conditions C and D. This suggests that the observed gains in hardness are more pronounced closer to the surface of the roller compared to the hardness measured at a higher indentation depth.

As shown by the hardness evolution data in *Figure 15*, hardness increased rapidly under conditions C and D (10-15%) during the first, approximately 22,000 contact cycles which corresponded to approximately 30 minutes of running-in. After this rapid increase, hardness appeared to reach a steady-state almost immediately. Condition B exhibited modest gains in hardness at about 44,000 contact cycles closer to the surface

while condition A showed insignificant changes. The hardness gains at the higher indentation depth for these conditions (*Figure 15b*) were insignificant.

Figure 16 focuses on the hardness gains experienced under each condition in the first 30 minutes by displaying the baseline (H_0) average hardness with the relative hardness gains achieved after approximately 22,000 contact cycles (H_{30}). Comparing conditions A to C and B to D show how increasing the initial composite surface roughness resulted in greater hardness gains as opposed to the comparison of conditions A to B and C to D which result in a less significant increase in hardness when the contact pressure is increased. Increasing the roughness could have contributed to an increased frequency of asperity collisions between the adjacent surfaces, resulting in an increase in plastic deformation. Work hardening can occur as a result of this plastic deformation, contributing to the increase in hardness observed. Another factor which could have contributed to the gains in hardness is the formation of a ZDDP tribofilm. Kalin et al. showed a ZDDP tribofilm on DIN 100Cr5 steel had a measured hardness of about 245 HV after a 25-minute test duration [73]. Consequently, the potential effect any tribofilm had on the resulting hardness gains for our samples was analyzed.

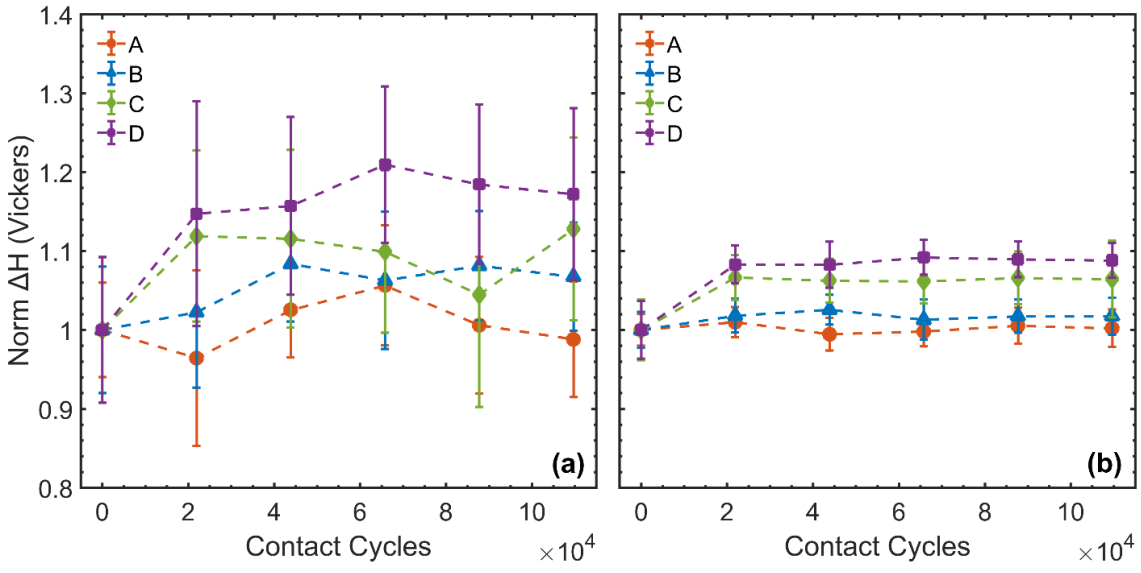

Figure 15. (a) Evolution of hardness under conditions A–D using 50-gf indenter load. (b) Evolution of hardness under conditions A-D using 500-gf indenter load. Error bars represent a 90% confidence interval.

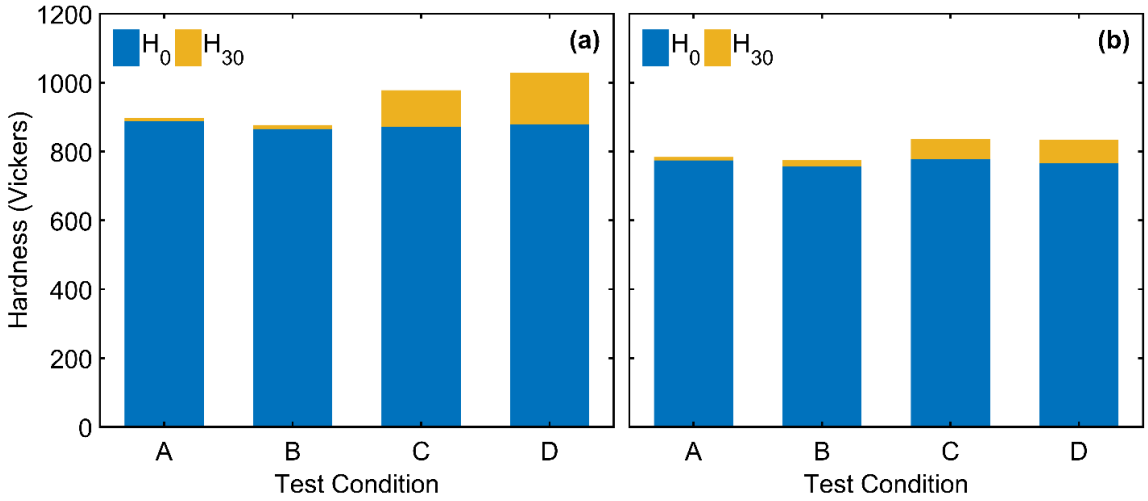

Figure 16. (a) Hardness under conditions A–D measured before testing (H_0) and after running-in for about 22,000 contact cycles or 30 minutes (H_{30}) using 50-gf indenter load. (b Hardness under conditions A–D measured before testing (H_0) and after running-in for about 22,000 contact cycles or 30 minutes (H_{30}) using 500-gf indenter load

Tribofilm Development

In order to determine the impact of tribofilm development on the evolution of hardness, a roller from each test condition was analyzed after 150 minutes of running-in using EDS to determine the existence of ZDDP tribofilm. The relative peaks of zinc, phosphorus, and sulfur were used to indicate the presence of ZDDP tribofilm growth. *Figure 17* shows the backscattered images from inside the wear zone for samples run under condition A to D. The darker regions correspond to the presence of tribofilm. It can be observed that the tribofilms are present on localized regions and are not uniform across the wear track. *Figure 18* shows EDS data collected from those regions. For comparison, EDS data was taken outside the wear zone which showed no trace of ZDDP for all conditions. *Figure 18* shows no peaks of zinc or phosphorus for condition A, suggesting the absence of a tribofilm under that condition. A small level of sulfur was observed which was most likely due to the presence of sulfur in the steel. For condition C, significant peaks of zinc, phosphorus, and sulfur were observed suggesting that condition C was highly conducive to the formation of a tribofilm. For conditions B and D, relatively small peaks were observed on specific dark spots indicated in *Figure 17*. For

the samples run under conditions B and D, the darker regions and spots might be attributed to inhomogeneous tribofilm growth as stated by Spikes [49]. Due to the cleaning procedure using isopropyl alcohol prior to analysis, it is unlikely the localized levels of zinc, phosphorus, and sulfur are due to lubricant trapped within the surface of the roller. Based on the isolated areas of zinc, phosphorus, and sulfur found under test conditions B and D, the higher contact pressure may remove enough of the surface layer material to prevent a tribofilm from developing. For condition A, the lower composite surface roughness and contact pressure conditions may reduce the interaction between the adjacent surfaces and do not promote for tribofilm development. In addition, the lambda ratio for condition A was the highest of any test (*Table 7*), suggesting the surfaces were more sufficiently lubricated. Tribofilms do not develop if the thickness of the lubricant is significantly greater than the surface roughness [49].

The data suggests the most favorable condition for tribofilm growth appeared to be condition C because of the relatively high levels of zinc, phosphorus, and sulfur and a more homogenous surface coverage. Condition C was chosen further analyze if the tribofilm growth affected the measured surface hardness.

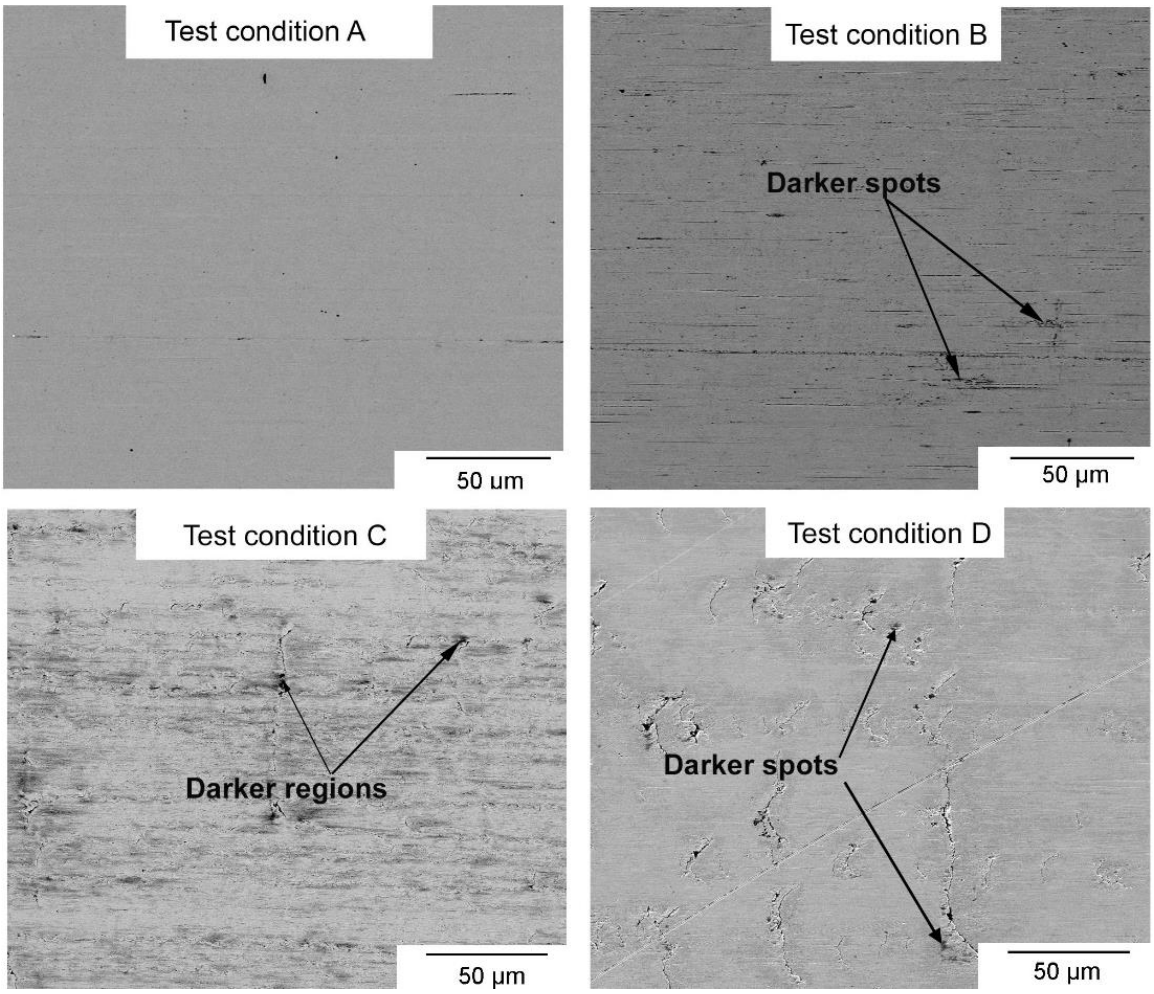

Figure 17. Backscatter images inside wear track for conditions A-D. Dark regions indicate areas of tribofilm.

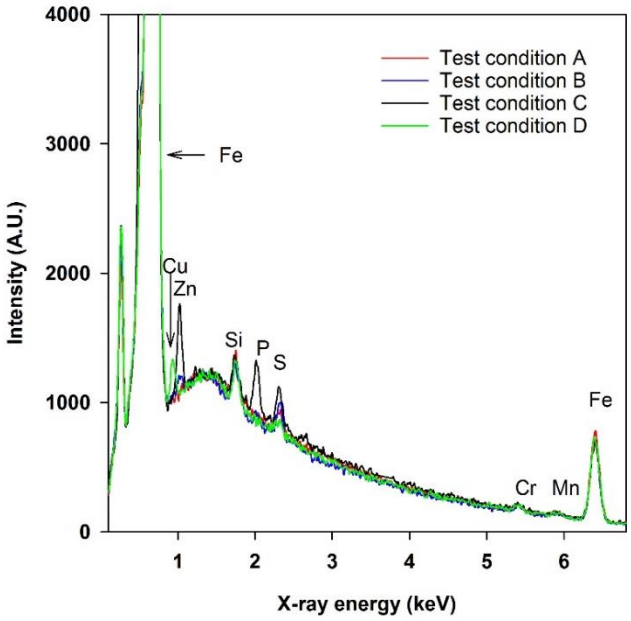

Figure 18. EDS data form inside the wear zone for each of the conditions. Tests used lubricant with ZDDP additive.

To observe the evolution of tribofilm growth and hardness more closely, one test under condition C was repeated to analyze how the tribofilm evolved throughout the course of running-in. Intermittent EDS measurements were performed at 15-minute, 30-minute, and 150-minute intervals. A control test was performed using Group II Base Oil without the ZDDP anti-wear additive, referred to as condition E.

Figure 20 shows the EDS spectrum data at intervals throughout running-in of conditions C and E. As one would expect, for condition E, the lack of zinc, phosphorus, and sulfur observed at every interval confirmed the absence of a tribofilm. By contrast, test condition C showed some levels of zinc, phosphorous, and sulfur after only 15-minutes (~11,000 contact cycles), indicating the formation of a tribofilm. This relatively rapid development of tribofilm has also been reported by Parsaeian et al. [62]. After about 22,000 contact cycles (30-minutes) of running-in, tribofilm growth stabilized as seen in the relative peaks after 30-minutes and 150-minutes of running-in. Consistent with other studies like that of Gosvami et al. [69], the tribofilm growth under condition C formed patchy features indicated as darker region or zones in *Figure 19*. The EDS measurements of these darker zones indicated a greater intensity of zinc, phosphorus,

and sulfur than what was observed from whole region (*Figure 20*) and the intensity of those elements increased with the number of contact cycles, suggesting tribofilm growth in these localized regions.

The hardness evolution data from conditions C and E are compared in *Figure 21*. The evolutions of the hardness profiles throughout the running-in of conditions C and E are similar, indicating the tribofilm formation had an insignificant impact on the observed hardness increase for the test duration.

One of the reasons the tribofilm may have had little effect on the observed hardness gains was due to its thickness relative to the depths at which hardness was measured. The indentation loads of 50-gf and 500-gf used in this study corresponded to depths of 1.4 µm and 4.8 µm respectively, which exceed the range of tribofilm thickness (50 - 200 nm) seen in literature [62,82]. Another reason the tribofilm may have had little effect on the observed hardness gains was because of its relative difference in hardness compared to the base material. 16MnCr5 steel's baseline hardness of about 880 HV at the 50-gf indentation load and about 770 HV at the 500-gf indentation load far exceed ZDDP tribofilm's hardness of about 245 HV as measured by Kalin et al. [73]. The typical thickness and hardness of tribofilms observed in literature suggest that it is unlikely ZDDP had a significant effect on the observed hardness gains in this study, rather, the primary contributor was from work hardening.

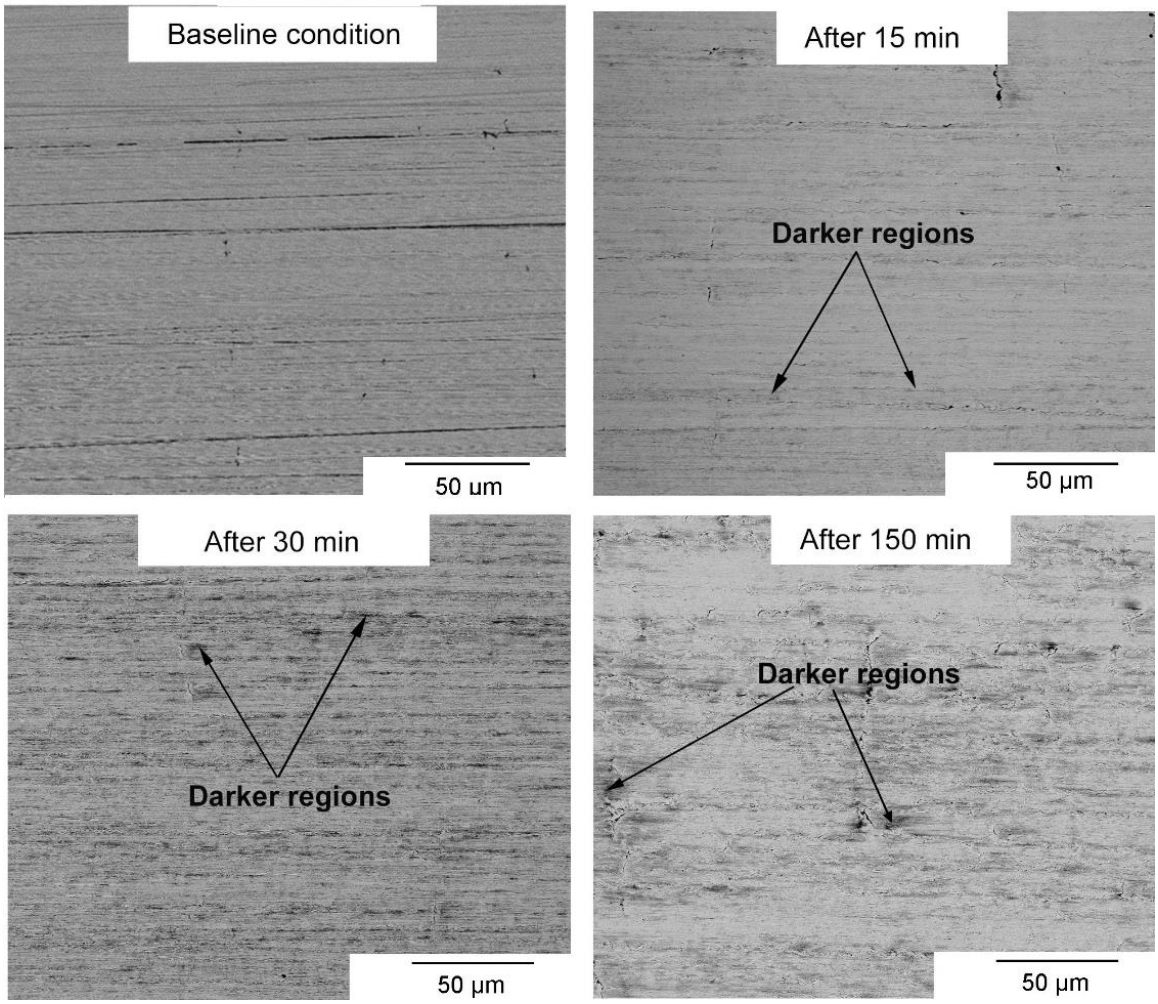

Figure 19. Backscatter image inside the wear track of roller throughout the evolution of tribofilm under condition C. Dark spots indicate regions of tribofilm formation.

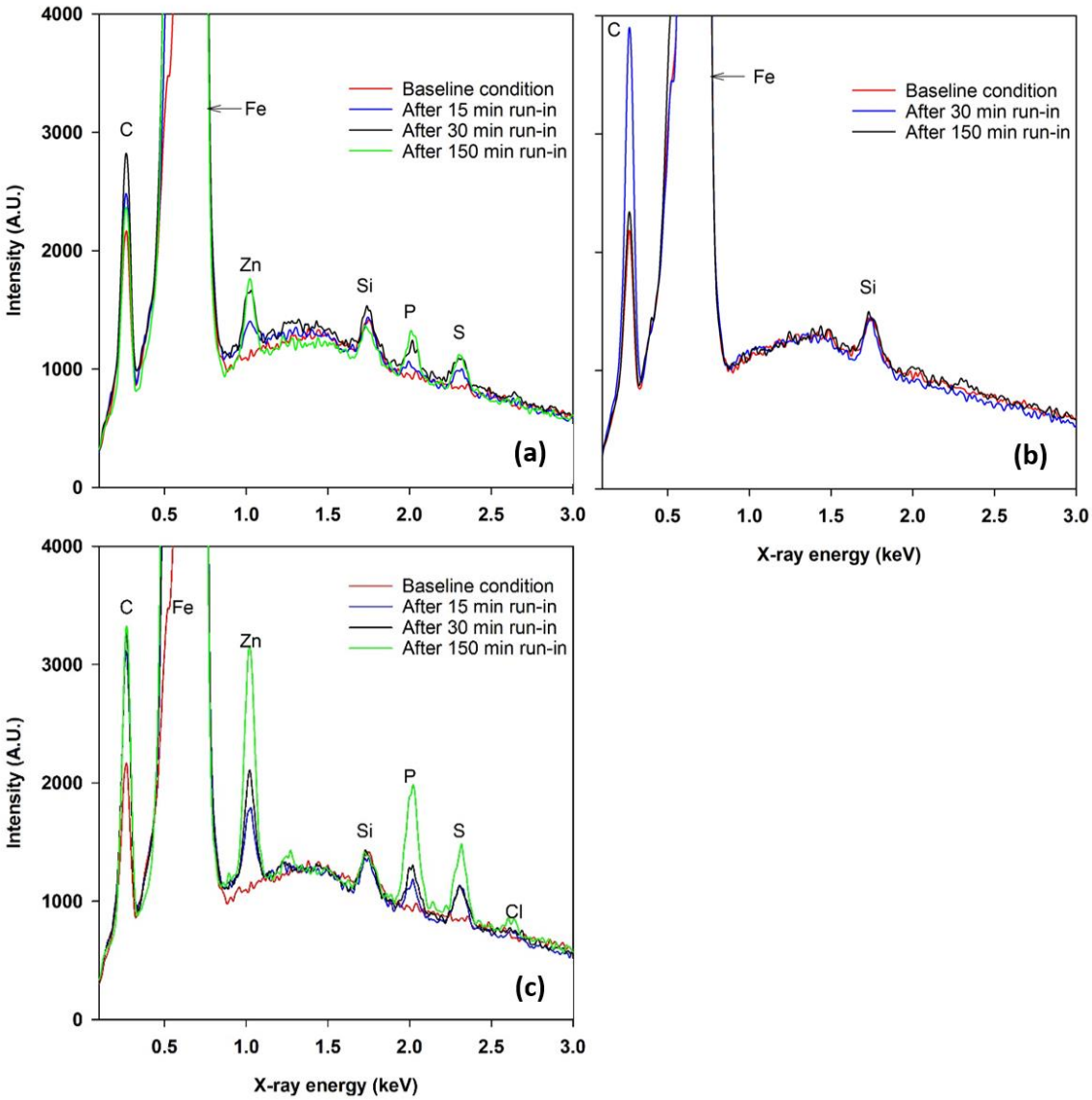

Figure 20. (a) EDS spectrum data measured inside the wear zone under condition C with ZDDP anti-wear additive. (b) EDS spectrum data measured inside the wear zone under condition E with Group II Base Oil (Absent ZDDP). (c) EDS spectrum data of dark regions/zones. Tribofilm formation increases with time in localized regions (c), but stabilizes after 30-min when averaged across wear track.

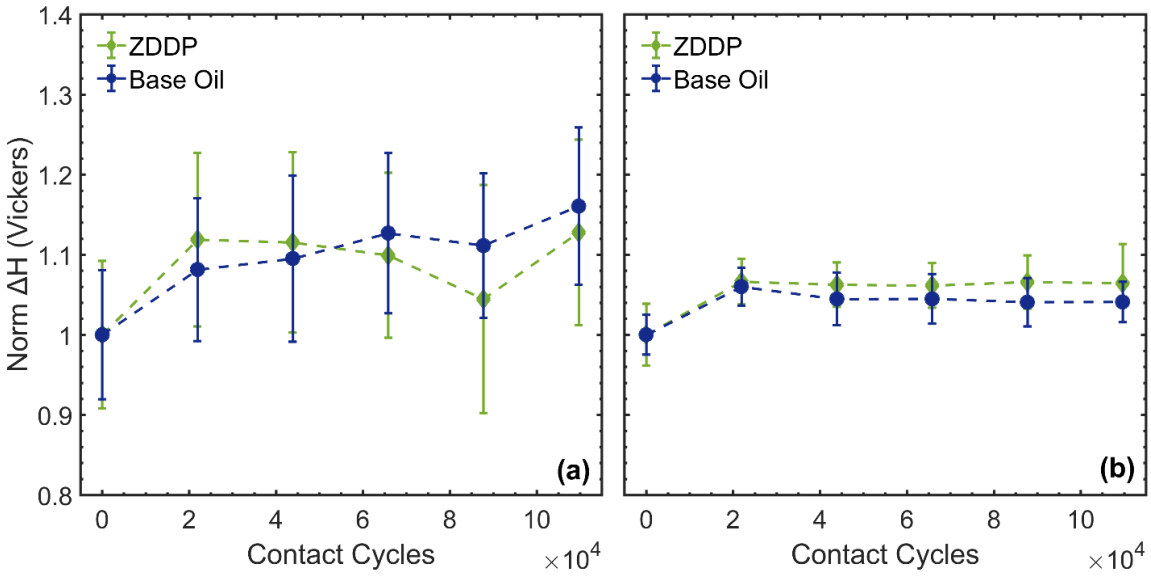

Figure 21. (a) Evolution of hardness under conditions C and E using 50-gf indenter load. (b) Evolution of hardness under conditions C and E using 500-gf indenter load. Error bars represent a 90% confidence interval.

Conclusions

The evolution of hardness and tribofilm growth during the running-in of 16MnCr5 steel was analyzed under varied contact pressure and initial composite roughness conditions. The results of this study showed:

(1) Hardness increased rapidly under all test conditions and generally stabilized after 22,000 contact cycles (30 minutes). The increase was more pronounced near the surface.

(2) Higher initial composite roughness produced greater gains in hardness than increasing the contact pressure.

(3) Tribofilm growth did not appear to have a significant effect on the measured hardness increase, suggesting the hardness gains are most likely due to the work hardening the surface layer undergoes during running-in.

CHAPTER 5. CONCLUSIONS AND FUTURE RESEARCH

Specific Findings and Limitations

The results the testing indicated that increasing the initial composite roughness and contact pressure conditions during the running-in of 16MnCr5 steel produced greater gains in hardness. The increase in hardness was attributed to the plastic deformations surfaces undergo during running-in which caused the surface layer to experience work hardening. Results suggest the development of a tribofilm from the ZDDP anti-wear lubricant additive had little to no effect on the measured hardness. Increasing initial composite roughness conditions appeared to have a more significant effect on the increase in hardness compared to the increase in contact pressure.

The hardness evolution data shows a rapid increase in hardness within the first 22,000 contact cycles or 30 minutes of running-in. This trend is primarily shown via conditions C and D which had higher initial composite roughness. The increase in hardness is more pronounced at the near-surface than the increase measured further into the depth of the material. This is consistent with the gradient in hardness which is typical for case-carburized steel. The relative difference in hardness also indicates more work hardening occurs at the surface than deeper into the material which was expected.

The roughness evolution data of Ra and Rz showed a rapid decrease in roughness within the first 22,000 cycles or 30 minutes of running-in. Conditions A and C, which had lower contact pressure, appeared to reach a steady-state whereas the higher contact pressure conditions of B and D appeared to steadily rise after the initial drop in roughness. This is most likely due to the increased contact pressure leading to a higher distribution of asperity contact which led to more rapid fatigue wear.

The surface roughness made hardness measurements difficult especially when measured at the near-surface and as test duration increase. The hardness measured at the near surface had much more variability in the data which was due to the small indentations made by the 50-gf indenter load and the geometry of the indent being easily skewed by surface features. The heterogeneity of the steel microstructure could

have also affected the measured hardness at the near-surface. It is recommended to use a higher indenter load like 100 to 200-gf to get a more consistent measurement of the hardness closer to the surface of the material.

The tribofilm analysis revealed growth was inconsistent across the test conditions. Condition C produced the most uniform tribofilm based on EDS analysis of the surface. The growth of tribofilm showed a similar trend to that of the hardness evolution in that it quickly grew within the first 22,00 cycles or 30 minutes of running before stabilizing. For conditions B and D, the localized presence of zinc, phosphorus, and sulfur might indicate the higher-pressure conditions prevented the tribofilm from developing because of the increased fatigue wear under those tests. It is unclear why no tribofilm was measured under condition A, but it could be due to the lower interaction between surfaces because of the lower initial composite roughness and pressure condition.

Future Work

Future studies could take test samples run-in under the varying initial composite roughness and contact pressure conditions from this study and analyze the resulting residual stress profiles and levels of retained austenite. By sectioning the test samples, one could also analyze the microstructural differences inside and outside the wear zone. The author also recommends performing hardness testing on the near-surface using an indenter load between 100 and 200-gf to achieve a more consistent hardness measurement.

REFERENCES

[1] S.Q.A. Rizvi, Lubricant Additives, Ind. Lubr. Tribol. 25 (1973) 63–68. doi:10.1108/eb053039.

[2] R. Wiser, M. Bolinger, G. Barbose, N. Darghouth, B. Hoen, A. Mills, K.H. LaCommare, D. Millstein, D. Hansen, K. Porter, R. Widiss, M. Buckley, F. Oteri, A. Smith, S. Tegen, 2014 Wind Technologies Market Report, Berkeley, CA (United States), 2015. doi:10.2172/1155074.

[3] K. Kato, History of Tribology, UMI Research Press, New York, 2011. doi:10.2474/trol.6.ii.

[4] P.A. Pacholke, K.M. Marshek, Improved Worm Gear Performance With Colloidal Molybdenum Disulfide Containing Lubricants, Lubr. Eng. 43 (1987) 623–628.

[5] L. Xiao, A study on the effect of surface topography on rough friction in roller contact, Wear. 254 (2003) 1162–1169. doi:10.1016/S0043-1648(03)00329-6.

[6] T.T. Petry-Johnson, A. Kahraman, N.E. Anderson, D.R. Chase, An experimental investigation of spur gear efficiency, J. Mech. Des. 130 (2008) 62601. doi:10.1115/1.2898876.

[7] H. Xu, A. Kahraman, N.E. Anderson, D.G. Maddock, Prediction of Mechanical Efficiency of Parallel-Axis Gear Pairs, J. Mech. Des. 129 (2007) 58. doi:10.1115/1.2359478.

[8] S. Li, A. Kahraman, Micro-pitting fatigue lives of lubricated point contacts: Experiments and model validation, Int. J. Fatigue. 48 (2013) 9–18. doi:10.1016/j.ijfatigue.2012.12.003.

[9] M. Yoshizaki, T. Hashimoto, C. Kasamatsu, Effect of Abnormal Surface Layer on Tooth Surface Strength Increase of Gas Carburized Gears, Tribol. Trans. 46 (2003) 83–94. doi:10.1080/10402000308982604.

[10] M. Sosa, U. Sellgren, S. Björklund, U. Olofsson, In situ running-in analysis of ground gears, Wear. 352–353 (2016) 122–129. doi:10.1016/j.wear.2016.01.021.

[11] R.C. Martins, N.F.R. Cardoso, H. Bock, A. Igartua, J.H.O. Seabra, Power loss performance of high pressure nitrided steel gears, Tribol. Int. 42 (2009) 1807–1815. doi:10.1016/j.triboint.2009.03.006.

[12] S. Kalpakjian, Manufacturing Processes for Engineering Materials, 2nd ed., Addison-Wesley, 1985. doi:10.1007/BF02833667.

[13] Y.B. Guo, M.E. Barkey, Modeling of rolling contact fatigue for hard machined components with process-induced residual stress, Int. J. Fatigue. 26 (2004) 605–613. doi:10.1016/j.ijfatigue.2003.10.009.

[14] Q. Chen, G.T. Hahn, C.A. Rubin, V. Bhargava, The influence of residual stresses on rolling contact mode II driving force in bearing raceways, Wear. 126 (1988) 17–30. doi:10.1016/0043-1648(88)90106-8.

[15] P.J. Blau, On the nature of running-in, Tribol. Int. 38 (2005) 1007–1012. doi:10.1016/j.triboint.2005.07.020.

[16] L. Berthe, P. Sainsot, A.A. Lubrecht, M.C. Baietto, Plastic deformation of rough rolling contact: An experimental and numerical investigation, Wear. 312 (2014) 51–57. doi:10.1016/j.wear.2014.01.017.

[17] J. Burbank, M. Woydt, Optimization of pre-conditioned cold work hardening of steel alloys for friction and wear reductions under slip-rolling contact, Wear. 350–351 (2016) 141–154. doi:10.1016/j.wear.2016.01.011.

[18] PCS Instruments, MPR (Micro Pitting Rig), (2017). http://pcs-instruments.com/product/mpr-micro-pitting-rig/.

[19] H.E. Boyer, Case Hardening of steel, ASM International, 1987.

[20] M. a. Klecka, G. Subhash, N.K. Arakere, Microstructure–Property Relationships in M50-NiL and P675 Case-Hardened Bearing Steels, Tribol. Trans. 56 (2013) 1046–1059. doi:10.1080/10402004.2013.818393.

[21] K. Burkart, H. Bomas, H.W. Zoch, Fatigue of notched case-hardened specimens of steel SAE 5120 in the VHCF regime and application of the weakest-link concept, Int. J. Fatigue. 33 (2011) 59–68. doi:10.1016/j.ijfatigue.2010.07.006.

[22] C.F. Yang, L.H. Chiu, J.K. Wu, Effects of carburization and hydrogenation on the impact toughness of AISI 4118 steel, Surf. Coatings Technol. 73 (1995) 18–22. doi:10.1016/0257-8972(94)02357-3.

[23] G. Stachowiak, A. Batchelor, Engineering Tribology, 4th ed., Butterworth-Heinemann, Boston, 2013. doi:10.1016/0301-679X(94)90034-5.

[24] P.J. Blau, Interpretations of the Friction and Wear Break-in Behavior in Metals in Sliding Contact., Wear. 71 (1981) 29–43. doi:10.1016/0043-1648(81)90137-X.

[25] S.M. Hsu, R.G. Munro, M.C. Shen, R.S. Gate, Run-in Process, in: G.W. Stachowiak (Ed.), Wear Mater. Mech. Pract., 1st ed., John Wiley & Sons Inc., London,Uk, 2005: pp. 37–69.

[26] E.J. Abbott, F.A. Firestone, Specifying surface quality- A method based on accurate measurement and comparison, Mech. Eng. 55 (1933) 569–577.

[27] J.D. Summers-Smith, A tribology casebook: a lifetime in tribology, Wiley, 1997. http://books.google.nl/books?id=esIeAQAAIAAJ.

[28] A. van Beek, Advanced engineering design : lifetime performance and reliability, 5th ed., TU Delft, 2006. http://adsabs.harvard.edu/abs/2006aedl.book.....V.

[29] S.K. Roy Chowdhury, H. Kaliszer, G.W. Rowe, An analysis of changes in surface topography during running-in of plain bearings, Wear. 57 (1979) 331–343. doi:10.1016/0043-1648(79)90107-8.

[30] B. Jacobson, Thin film lubrication of real surfaces, Tribol. Int. 33 (2000) 205–210. doi:10.1016/S0301-679X(00)00032-3.

[31] S. Andersson, Initial wear of gears, Tribol. Int. 10 (1977) 206–210. doi:10.1016/0301-679X(77)90021-4.

[32] S. Akbarzadeh, M.M. Khonsari, On the Prediction of Running-In Behavior in Mixed-Lubrication Line Contact, J. Tribol. 132 (2010) 32102. doi:10.1115/1.4001622.

[33] D.J. Whitehouse, Handbook of Surface and Nanometrology, CRC Press, 2003. doi:10.1887/0750305835.

[34] D.J. Whitehouse, J.F. Archard, The Properties of Random Surfaces of Significance in their Contact, Proc. R. Soc. A Math. Phys. Eng. Sci. 316 (1970) 97–121. doi:10.1098/rspa.1970.0068.

[35] S. Akbarzadeh, M.M. Khonsari, On the optimization of running-in operating conditions in applications involving EHL line contact, Wear. 303 (2013) 130–137. doi:10.1016/j.wear.2013.01.098.

[36] A. Clarke, I.J.J. Weeks, R.W. Snidle, H.P. Evans, Running-in and micropitting behaviour of steel surfaces under mixed lubrication conditions, Tribol. Int. 101 (2016) 59–68. doi:10.1016/j.triboint.2016.03.007.

[37] H. Hertz, Ueber die Ber??hrung fester elastischer K??rper, J. Fur Die Reine Und Angew. Math. 1882 (1882) 156–171. doi:10.1515/crll.1882.92.156.

[38] I.S. Al-Tubi, H. Long, J. Zhang, B. Shaw, Experimental and analytical study of gear micropitting initiation and propagation under varying loading conditions, Wear. 328–329 (2015) 8–16. doi:10.1016/j.wear.2014.12.050.

[39] J. a. Greenwood, J.B.P. Williamson, Contact of Nominally Flat Surfaces, Proc. R. Soc. A Math. Phys. Eng. Sci. 295 (1966) 300–319. doi:10.1098/rspa.1966.0242.

[40] E. Deeg, New algorithms for calculating Hertzian stresses, deformations, and contact zone parameters, AMP J. Technol. 2 (1992) 14–24. http://scholar.google.com/scholar?hl=en&btnG=Search&q=intitle:New+Algorithms+for+Calculating+Hertzian+Stresses+,+Deformations+,+and+Contact+Zone+Parameters#0.

[41] F. Hirano, N. Kuwano, K. Ichimaru, Effect of work hardening during rolling contact on pitting of gear materials, Proc. Inst. Mech. Eng. 181 (1966) 85–93. doi:10.1243/PIME_CONF_1966_181_302_02.

[42] R.C. Dommarco, K.J. Kozaczek, P.C. Bastias, G.T. Hahn, C.A. Rubin, Residual stresses and retained austenite evolution in SAE 52100 steel under non-ideal rolling contact loading, Wear. 257 (2004) 1081–1088. doi:10.1016/j.wear.2004.01.020.

[43] J.-H. Kang, R.H. Vegter, P.E.J. Rivera-Díaz-del-Castillo, Rolling contact fatigue in martensitic 100Cr6: Subsurface hardening and crack formation, Mater. Sci. Eng. A. 607 (2014) 328–333. doi:10.1016/j.msea.2014.03.143.

[44] A.N. Grubin, I.E. Vinogradova, Fundamentals of the hydrodynamic theory of lubrication of heavily loaded cylindrical surfaces, Central Scientific Institute for Technology and Mechanical Engineering, Moscow, 1949.

[45] D. Dowson, Elastohydrodynamic and micro-elastohydrodynamic lubrication, Wear. 190 (1995) 125–138. doi:10.1016/0043-1648(95)06660-8.

[46] T.E. Tallian, Competing failure modes in rolling contact, A S L E Trans. 10 (1967) 418–439. doi:10.1080/05698196708972201.

[47] K.L. Johnson, J.A. Greenwood, S.Y. Poon, A simple theory of asperity contact in elastohydro-dynamic lubrication, Wear. 19 (1972) 91–108. doi:10.1016/0043-1648(72)90445-0.

[48] K. Ito, J.M. Martin, C. Minfray, K. Kato, Formation Mechanism of a Low Friction ZDDP Tribofilm on Iron Oxide, Tribol. Trans. 50 (2007) 211–216. doi:10.1080/10402000701271010.

[49] H. Spikes, The history and mechanisms of ZDDP, Tribol. Lett. 17 (2004) 469–489. doi:10.1023/B:TRIL.0000044495.26882.b5.

[50] S. Soltanahmadi, A. Morina, M.C.P. van Eijk, I. Nedelcu, A. Neville, Tribochemical study of micropitting in tribocorrosive lubricated contacts: The influence of water and relative humidity, Tribol. Int. 107 (2017) 184–198. doi:10.1016/j.triboint.2016.11.031.

[51] J.F. Graham, C. Mccague, P.R. Norton, Topography and nanomechanical properties of tribochemical films derived from zinc dialkyl and diaryl dithiophosphates, Tribol. Lett. 6 (1999) 149–157. doi:10.1023/A:1019124026402.

[52] M. Aktary, M.T. McDermott, G.A. McAlpine, Morphology and nanomechanical properties of ZDDP antiwear films as a function of tribological contact time, Tribol. Lett. 12 (2002) 155–162. doi:10.1023/A:1014755123184.

[53] L. Taylor, H. Spikes, H. Camenzind, Film-Forming Properties of Zinc-Based and Ashless Antiwear Additives, in: Spec. Chem., 2000. doi:10.4271/2000-01-2030.

[54] L. Taylor, A. Dratva, H.A. Spikes, Friction and Wear Behavior of Zinc Dialkyldithiophosphate Additive, Tribol. Trans. 43 (2000) 469–479. doi:10.1080/10402000008982366.

[55] N.J. Mosey, T.K. Woo, M. Kasrai, P.R. Norton, G.M. Bancroft, M.H. Müser, Interpretation of experiments on ZDDP anti-wear films through pressure-induced cross-linking, Tribol. Lett. 24 (2006) 105–114. doi:10.1007/s11249-006-9040-9.

[56] G.W. Canning, M.L. Suominen Fuller, G.M. Bancroft, M. Kasrai, J.N. Cutler, G. De Stasio, B. Gilbert, Spectromicroscopy of tribological films from engine oil additives. Part I. Films from ZDDP's, Tribol. Lett. 6 (1999) 159–169. doi:10.1023/A:1019176110473.

[57] R.J. Bird, G.D. Galvin, The application of photoelectron spectroscopy to the study of e. p. films on lubricated surfaces, Wear. 37 (1976) 143–167. doi:10.1016/0043-1648(76)90188-5.

[58] R.J. Bird, R.C. Coy, J.F. Hutton, The Preparation and Nature of Surface Films from Zinc Dialkyldithiophosphate, A S L E Trans. 23 (1980) 121–130. doi:10.1080/05698198008982953.

[59] A. Tonck, J.M. Martin, P. Kapsa, J.M. Georges, Boundary lubrication with anti-wear additives: study of interface film formation by electrical contact resistance, Tribol. Int. 12 (1979) 209–213. doi:10.1016/0301-679X(79)90190-7.

[60] J.M. Palacios, Thickness and chemical composition of films formed by antimony dithiocarbamate and zinc dithiophosphate, Tribol. Int. 19 (1986) 35–39. doi:10.1016/0301-679X(86)90093-9.

[61] J.M. Palacios, Films formed by antiwear additives and their incidence in wear and scuffing, Wear. 114 (1987) 41–49. doi:10.1016/0043-1648(87)90014-7.

[62] P. Parsaeian, M.C.P. Van Eijk, I. Nedelcu, A. Neville, A. Morina, Study of the interfacial mechanism of ZDDP tribofilm in humid environment and its effect on tribochemical wear; Part I: Experimental, Tribol. Int. 107 (2017) 135–143. doi:10.1016/j.triboint.2016.11.012.

[63] R.D. Evans, G.L. Doll, C.H. Hager, J.Y. Howe, Influence of steel type on the propensity for tribochemical wear in boundary lubrication with a wind turbine gear oil, Tribol. Lett. 38 (2010) 25–32. doi:10.1007/s11249-009-9565-9.

[64] G.W. Stachowiak, Wear - Materials, mechanisms and practice, 2013. doi:10.1017/CBO9781107415324.004.

[65] I.. V. Kragelsky, M.N. Dobychin, V.S. Kombalov, Friction and wear: calculation methods, illustrate, Pergamon Press, Oxford, 1981.

[66] J.R. Miller, The Influence of Bearing Run-In on Lambda Calculations, in: 1990. doi:10.4271/901626.

[67] S. Akbarzadeh, M.M. Khonsari, Experimental and theoretical investigation of running-in, Tribol. Int. 44 (2011) 92–100. doi:10.1016/j.triboint.2010.09.006.

[68] A.C. Fischer-Cripps, Nanoindentation, 3rd ed., Springer New York, New York, NY, 2011. doi:10.1007/978-1-4419-9872-9.

[69] N.N. Gosvami, J.A. Bares, F. Mangolini, A.R. Konicek, D.G. Yablon, R.W. Carpick, Mechanisms of antiwear tribofilm growth revealed in situ by single-asperity sliding contacts, Science (80-.). 348 (2015) 102–106. doi:10.1126/science.1258788.

[70] J. Jelita Rydel, K. Pagkalis, A. Kadiric, P.E.J. Rivera-Díaz-del-Castillo, The correlation between ZDDP tribofilm morphology and the microstructure of steel, Tribol. Int. (2016) 0–1. doi:10.1016/j.triboint.2016.10.039.

[71] J. Schöfer, P. Rehbein, U. Stolz, D. Löhe, K.H. Zum Gahr, Formation of tribochemical films and white layers on self-mated bearing steel surfaces in boundary lubricated sliding contact, Wear. 248 (2001) 7–15. doi:10.1016/S0043-1648(00)00549-4.

[72] S.M. Ganechari, V.R. Kabadi, S.A. Kori, Study of surface roughness and hardness of low carbon nickel-chromium based alloy steels under high temperature (AISI sae8630, 3140 & 9310), in: Proc. Int. Conf. Work. Emerg. Trends Technol. - ICWET '11, ACM Press, New York, New York, USA, 2011: p. 1316. doi:10.1145/1980022.1980312.

[73] M. Kalin, E. Oblak, S. Akbari, Evolution of the nano-scale mechanical properties of tribofilms formed from low- and high-SAPS oils and ZDDP on DLC coatings and steel, Tribol. Int. 96 (2016) 43–56. doi:10.1016/j.triboint.2015.12.013.

[74] C. Locateli, R. Martins, J. Seabra, Evolution of tooth flank roughness during gear micropitting tests, Ind. Lubr. Tribol. 63 (2011) 211–212. doi:http://dx.doi.org/10.1108/00368791111101821.

[75] A. Bengtsson, A. Rönnberg, The absolute measurement of running-in, Wear. 109 (1986) 329–342. doi:10.1016/0043-1648(86)90276-0.

[76] Y.-R. Jeng, Z.-W. Lin, S.-H. Shyu, Changes of Surface Topography During Running-In Process, J. Tribol. 126 (2004) 620. doi:10.1115/1.1759344.

[77] O. Zwirlein, H. Schlicht, Rolling Contact Fatigue Mechanisms—Accelerated Testing Versus Field Performance, in: Roll. Contact Fatigue Test. Bear. Steels, ASTM International, 100 Barr Harbor Drive, PO Box C700, West Conshohocken, PA 19428-2959, n.d.: pp. 358-358–22. doi:10.1520/STP36149S.

[78] A.J. Caines, R.F. Haycock, J.E. Hillier, Automotive Lubricants Reference Book, Ind. Lubr. Tribol. 57 (2005) ilt.2005.01857aae.001. doi:10.1108/ilt.2005.01857aae.001.

[79] A.G. Papay, Antiwear and extreme-pressure additives in lubricants, Lubr. Sci. 10 (1998) 209–224. doi:10.1002/ls.3010100304.

[80] J.J. Wagner, A.D. Jenson, S. Sundararajan, The effect of contact pressure and surface texture on running-in behavior of case carburized steel under boundary lubrication, Wear. (2017). doi:10.1016/j.wear.2017.02.016.

[81] B.K. Sharma, A.J. Stipanovic, Pressure Viscosity Coefficient of Lubricant Base Oils As Estimated by Nuclear Magnetic Resonance Spectroscopy, Ind. Eng. Chem. Res. 41 (2002) 4889–4898. doi:10.1021/ie020360q.

[82] A.P. Voskamp, Material Response to Rolling Contact Loading, J. Tribol. 107 (1985) 359. doi:10.1115/1.3261078.

[83] J. Jelita Rydel, R.H. Vegter, P.E.J. Rivera-Díaz-Del-Castillo, Tribochemistry of bearing steels: A new AFM method to study the material-tribofilm correlation, Tribol. Int. 98 (2016) 74–81. doi:10.1016/j.triboint.2016.01.055.